Role of D-Valine Residues in the Antitumor Drug Actinomycin D: Replacement of D-Valines with Other D-Amino Acids Changes the DNA Binding Characteristics and Transcription Inhibitory Activities†

Wenhua Chu, Miho Shinomiya,§ Kazuyo Y. Kamitori, Shigehiro Kamitori, Robert G. Carlson, Robert F. Weaver, and Fusao Takusagawa*

Contribution from the Departments of Chemistry and Biochemistry, University of Kansas, Lawrence, Kansas 66045-0046

Received February 14, 1994®

Abstract: D-valine analogues of the antitumor drug actinomycin D, in which D-valine residues were replaced with D-threonine, D-tyrosine, D-phenylalanine, and D-*O*-methyltyrosine residues, have been totally synthesized. The crystal structure of the D-*O*-methyltyrosine analogue has been determined ($a = b = 21.352(6)$, $c = 44.525(9)$ Å; space group $P4_12_12$; $R = 0.19$ for 803 out of 1114 reflections at 1.8 Å resolution data). Replacements of D-valines did not change the overall conformation of the molecule, and the substituted groups were located on the side opposite to the DNA binding site, suggesting that the analogues can bind intercalatively at 5′-GC-3′ sequences of DNA like actinomycin D does. In the crystals, the analogue molecules constitute a tight dimer, and a pair of stacked chromophores of the dimer was further sandwiched by two methoxyphenyl groups of neighboring molecules. These strong aromatic–aromatic stacking forces among the molecules appear to reduce very much the water solubility of the aromatic analogues. The characteristics of binding of the analogues to various DNA's including $d(GAAGCTTC)_2$, $d(GTTGCAAC)_2$, poly(dA-dT), poly(dG-dC), and calf thymus DNA have been examined by using the visible spectrum methods. Difference spectra of actinomycin D and the analogues with oligonucleotides indicated that the analogues bind intercalatively to the DNA, as actinomycin D does, but the association constants were reduced to approximately one-half that of actinomycin D. The spectra of the aromatic analogues titrated with calf thymus DNA indicated that the aromatic analogues bound somehow differently to the longer DNA's. A simple profile analysis of the spectra suggested that the aromatic analogues bound to calf thymus DNA not only with intercalation, as actinomycin D does, but also with side binding. Nevertheless, the association constants of the aromatic analogues to calf thymus DNA with the intercalation mode were found to be quite similar to those of the short oligonucleotides. This conclusion has been supported by the melting behaviors of the DNA with the aromatic analogues, in which the melting curves of the analogues were superimposable on the melting curve of DNA with actinomycin D, suggesting that the aromatic analogue molecules were intercalated into the DNA. The inhibitory activities of actinomycin D and analogues on RNA polymerase *in vitro* were examined using calf thymus DNA and *E. coli* RNA polymerase. All actinomycin D analogues severely inhibited RNA synthesis at relatively low drug concentrations. In general, inhibitory activities of the analogues on the RNA synthesis were found to be correlated with those of DNA binding characteristics. However, the analogue in which D-phenylalanine replaced D-valines inhibited RNA synthesis more strongly than actinomycin D itself, but this analogue bound to the DNA's much more weakly than actinomycin D. In this study, the D-valine residues in the cyclic depsipeptides of actinomycin D were found not to be directly involved in DNA binding, but this amino acid residue was found to be an important biological modulator of the antibiotic. Although the D-valine is a hydrophobic amino acid residue, this amino acid residue appears to play an important role in increasing the water solubility of the antibiotic. Replacements of D-valine residues reduced drastically the water solubility of the analogues, and consequently, this physical character of the analogues reduced their capacities for binding to DNA. As a result, the biological activities of the analogues were generally decreased.

Introduction

Actinomycin D (AMD) contains a planar phenoxazone ring as well as two cyclic depsipeptides, as shown in Figure 1, and is best known for its effectiveness as an inhibitor of transcription.[1-3] It has been employed clinically as an antitumor agent for treatment of highly malignant tumors such as Wilms tumor[4] and gestational choriocarcinoma.[5,6] Currently AMD is used with combinations of other antitumor drugs to treat high-risk tumors. For example, the EMA/CV regimen (Etoposide, methotrexate, AMD, cyclophosphamide, vincristine) has been used to treat gestational trophoblastic tumors[7] and the VAC regimen (vincristine, AMD, cyclophosphamide) and VAB-6 (vinblastine, AMD, bleomycin) are for treatment of childhood germ cell tumors.[8,9] A recent study by Wheeler *et al.*[10] suggested that AMD has not only transcription inhibitory activity but also other biological activities.

† Syntheses by W. Chu, DNA binding by M. Shinomiya, RNA synthesis inhibition by K. Y. Kamitori, and X-ray structure determination by S. Kamitori have been carried out.

§ Present address: Department of Chemistry, Shyonan Institute of Technology, Fujisawa, Japan.

* To whom correspondence should be addressed.

® Abstract published in *Advance ACS Abstracts,* July 15, 1994.

(1) Goldberg, J. H.; Friedman, P. A. *Annu. Rev. Biochem.* **1971**, *40*, 775–810.

(2) Kersten, H.; Kersten, W. Actinomycin. *Inhibitors of Nucleic Acid Synthesis*; Springer Verlag: Berlin, 1974; pp 40–66.

(3) Waring, M. Inhibitors of nucleic acid synthesis. In *The Molecular Basis of Antibiotics Action*; Gale, F., *et al.*, Eds.; Wiley: London, 1981; pp 258–401.

(4) Farber, S. J. *JAMA, J. Am. Med. Assoc.* **1966**, *198*, 826–836.

(5) Lewis, J. L. *Cancer* **1972**, *30*, 1517–1521.

(6) Schink, J. C.; Singh, D. K.; Rademaker, A. W.; Miller, D. S.; Lurain, J. R. *Obstet. Gynecol.* **1992**, *80*, 817–820.

(7) Newlands, E. S.; Bagshawe, K. D.; Begent, R. H. J.; Rustin, G. J. S.; Holden, L. *Br. J. Obstet. Gynaecol.* **1991**, *98*, 550–557.

(8) Marina, N.; Fontanesi, J.; Kun, L.; Rao, B.; Jenkins, J. J.; Thompson, E. I.; Etcubanas, E. *Cancer* **1992**, *70*, 2568–2575.

(9) Nakamura, E.; Kaneko, Y.; Takenawa, J.; Sasaki, M. *Acta Urol. Jpn.* **1992**, *38*, 913–918.

(10) Wheeler, H. R.; Rockett, E. J.; Clark, I.; Geczy, C. L. *Clin. Exp. Immunol.* **1991**, *86*, 304–310.

0002-7863/94/1516-7971$04.50/0

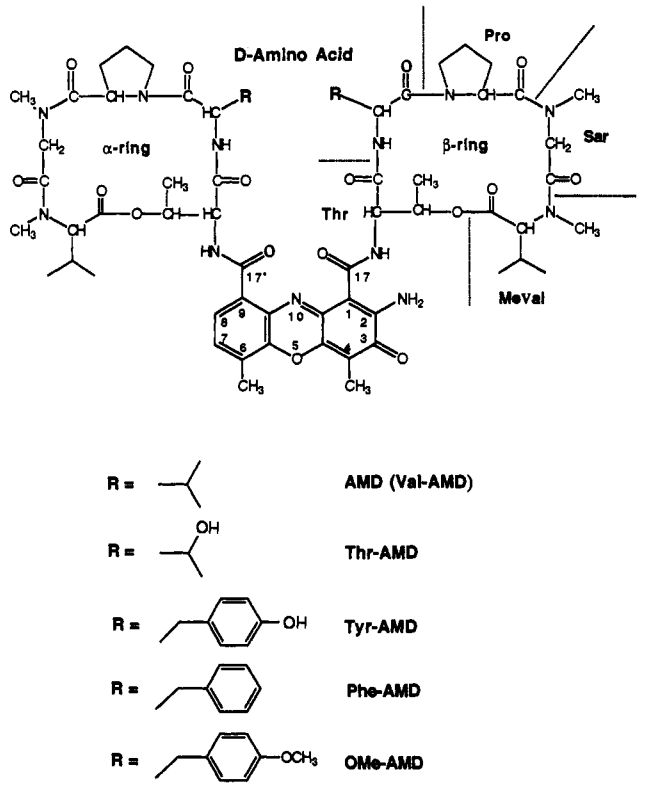

Figure 1. Molecular formulas of AMD and AMD analogues.

They reported that AMD directly induced procoagulant activity on the malignant monocytoid cell line WEHI 265 and acted synergistically with lipopolysaccharide to enhance macrophage membrane-bound procoagulant activity on both WEHI 265 cells and thioglycolate-induced peritoneal exudate macrophages. Accordingly, AMD may act by altering the synthesis of regulatory proteins controlling tissue factor and tumor necrosis factor α transcription.

In addition to its biological importance, AMD has been studied as a model of the drugs which bind to DNA sequence-specifically. Müller and Crothers investigated the binding properties of AMD analogues by hydrodynamic, kinetic, and thermodynamic studies.[11] They have shown that drugs bind preferentially into the 5′-GC-3′ steps of double-stranded DNA by intercalation. The 5′-GC-3′ binding preference was confirmed by X-ray crystallographic and 2D-NMR studies.[12-17] Several thermodynamic investigations have established that enthalpies of AMD binding to DNA provide small negative values compared with those of other intercalators such as ethidium bromide and daunomycin, which bind to DNA with large enthalpic driving forces.[18-22] It has been proposed that AMD binding occurs with a very large entropic driving force resulting from changes of hydrations around DNA.[20,23,24] This characteristic of thermodynamic behavior of AMD may relate to the unusual solubility of AMD in water, which exhibits a large negative temperature dependence. A large and negative solution entropy has been found at low temperatures.[20]

Recently, it has been revealed by various biological analyses, *i.e* footprinting and transcription assay, that neighboring and next-neighboring bases of 5′-GC-3′ steps affect the binding of AMD to DNA.[25-27] Further, Chen studied the DNA binding affinity of AMD by using a series of oligonucleotides containing different XGCY sites.[28,29] He reported that AMD binding strength decreases in the order of TGCA > CGCG > AGCT ≫ GGCC. On the other hand, several new binding sequences which contain no 5′-GC-3′ bases have been reported.[18,19] In particular, Snyder *et al.* propose a high-affinity, sequence-dependent DNA binding made different from the classic binding to 5′-GC-3′ steps.[18]

Although AMD possesses valuable biological activities, its clinical usefulness is limited by its extreme cytotoxicity. However, there is no general correlation between the antibacterial potency and antitumor activity.[30] Thus, if the AMD structure can be modified to reduce its cytotoxicity while retaining most of its antitumor activity, such an analogue would be a better antitumor agent. Analogues of AMD have been produced by directed biosynthesis, partial synthesis, and total synthesis.[30-32] In many cases, replacements of amino acid residues in the cyclic depsipeptides of AMD have been found to render such analogues inactive or less active. However, a few analogues have been shown very promising results. For example, Me-Leu$_5$-AMD (*N*-methylvaline at the C-terminal is replaced with *N*-methylleucine) displays less antimicrobial activity but higher antitumor activity than AMD itself *invitro*.[33] In the DNA–AMD complex structures determined recently by the X-ray diffraction method,[14,34] the isopropyl groups of the D-valine residues are pointed to the outside of the complex, and thus these groups are considered not to participate in interaction with DNA. Therefore, AMD analogues, in which the D-valine residues are replaced with other D-amino acid residues, are expected to bind to DNA as strongly as AMD does. If AMD inhibits RNA synthesis by just binding intercalatively to DNA, these AMD analogues will inhibit RNA synthesis as strongly as AMD does. However, if the cyclic depsipeptides of AMD play an unexpected role in inhibition of RNA synthesis, replacement of the D-valine residues with other residues would affect the inhibition activities of the AMD analogues.[35] Although synthetic analogues in which the D-valines were replaced by D-alanine or D-leucine were reported to be biologically inactive in late 1960,[36] we have synthesized several AMD analogues with the D-valine replaced with aromatic D-amino acid residues. Here we report the effects on DNA binding characteristics and

(11) Müller, M.; Crothers, D. M. *J. Mol. Biol.* **1968**, *35*, 251–290.
(12) Sobell, H. M.; Jain, S. C.; Sakore, T. D.; Nordman, C. E. *Nature, New Biol.* **1971**, *231*, 200–205.
(13) Takusagawa, F.; Dabrow, M.; Neidle, S.; Berman, H. M. *Nature* **1982**, *296*, 466–469.
(14) Kamitori, S.; Takusagawa, F. *J. Mol. Biol.* **1992**, *255*, 445–456.
(15) Brown, S. C.; Mullis, K.; Levenson, C.; Shafer, R. H. *Biochemistry* **1984**, *23*, 403–408.
(16) Zhou, N.; James, T. L.; Shafer, R. H. *Bichemistry* **1989**, *28*, 5231–5239.
(17) Liu, X.; Chen, H.; Patel, D. J. *J. Biomol. NMR* **1991**, *1*, 323–347.
(18) Snyder, J. G.; Hartman, N. G.; D'Estantoit, B. L.; Kennard, O.; Remeta, D. P.; Breslauer, K. J. *Proc. Natl. Acad. Sci. U.S.A.* **1989**, *86*, 3968–3972.
(19) Bailey, S. A.; Graves, D. E.; Rill, R.; Marsch, G. *Biochemistry* **1993**, *32*, 5881–5887.
(20) Gallert, M.; Smith, C. E.; Neville, D.; Felsenfeld, G. *J. Mol. Biol.* **1965**, *11*, 445–457.
(21) Chou, W. Y.; Marky, L. A.; Zaunczkowski, D.; Breslauer, K. J. *J. Biomol. Struct. Dyn.* **1987**, *5*, 345–359.
(22) Breslauer, K. J.; Remeta, D. P.; Chou, W.-Y.; Rerrante, R.; Curry, J.; Zaunczkoski, D.; Snyder, J. G.; Marky, L. A. *Proc. Natl. Acad. Sci. U.S.A.* **1987**, *84*, 8922–8926.
(23) Ginell, S. L.; Lessinger, L.; Berman, H. M. *Biopolymers* **1988**, *27*, 843–864.
(24) Marky, L. A.; Snyder, J. G.; Remeta, D. P.; Breslauer, K. *J. Biomol. Struct. Dyn.* **1983**, *1*, 487–507.
(25) Scramrov, A. V.; Beabealashvilli, R. Sh. *FEBS Lett.* **1983**, *164*, 97–101.
(26) Goodismen, J.; Rehfuss, R.; Ward, B.; Dabrowiak, J. C. *Biochemistry* **1992**, *31*, 1046–1058.
(27) Phillips, D. R.; Crothers, D. M. *Biochemistry* **1986**, *25*, 7355–7362.
(28) Chen, F.-M. *Biochemistry* **1988**, *27*, 6393–6397.
(29) Chen, F.-M. *Biochemistry* **1992**, *31*, 6223–6228.
(30) Meienhofer, J.; Atherton, E. Structure-activity relationships in the actinomycins. In *Structure-Activity Relationships among the Semisynthetic Antibiotics*; Perlman, D., Ed.; Academic Press: New York, San Francisco, London, 1977; pp 427–529.
(31) Mauger, A. B. The actinomycins. In *Topics in Antibiotic Chemistry*; Sammes, P. G., Ed.; E. Horwood: Chichester, 1980; pp 224–306.
(32) Mauger, A. B. Actinomycins. In *The Chemistry of Antitumor Agents*; Wilman, E. V., Ed.; Blackie & Son: Glasgow, 1990; pp 403–409.
(33) Mauger, A. B.; Stuart, O. A.; Katz, E. *J. Med. Chem.* **1991**, *34*, 1297–1301.
(34) Kamitori, S.; Takusagawa, F. *J. Am. Chem. Soc.* **1994**, *116*, 4154–4165.
(35) Takusagawa, F. *J. Antibiot.* **1985**, *38*, 1596–1604.
(36) Brockmann, H.; Lackner, H. *Chem. Ber.* **1968**, *101*, 1312.
(37) Chu, W.; Kamitori, S.; Shinomiya, M.; Carlson, R. G.; Takusagawa, F. *J. Am. Chem. Soc.* **1994**, *116*, 2243–2253.

Scheme 1. Syntheses of AMD Analogues Containing D-Phe and D-MeOTyr in Place of D-Val

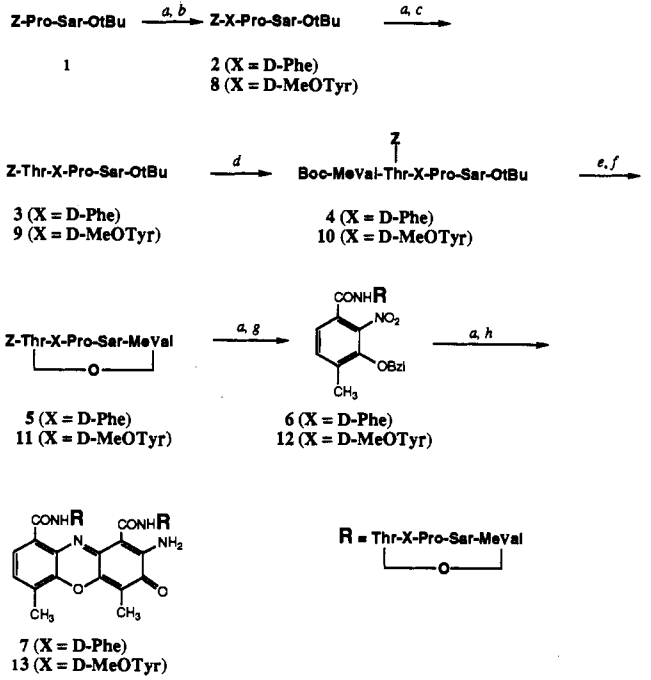

[a] (a) Pd/C, H_2; (b) Z-D-Phe-OH or Z-D-MeOTyr-OH, DCC; (c) Z-Thr-OH, DCC; (d) Boc-MeVal, DCC, DMAP; (e) F_3CCOOH; (f) BOP-Cl, $N(Et)_3$; (g) BMNBCA, DCC; (h) $K_3Fe(CN)_6$, pH 7.12.

transcription inhibitory activities upon replacing the D-valine residues of AMD with other D-amino acid residues.

Results and Discussion

Synthesis. AMD analogues in which D-valine residues were replaced with D-threonines (Thr-AMD), D-tyrosines (Tyr-AMD), D-phenylalanines (Phe-AMD), and D-*O*-methyltyrosines (OMe-AMD) have been synthesized by a slightly modified procedure of Mauger.[33] Thr-AMD is a known compound,[33] while the others are new compounds. The synthetic procedures for Phe-AMD and OMe-AMD are shown in Scheme 1, and the procedure for Tyr-AMD is given in Scheme 2. The X-ray structure of OMe-AMD has been carried out to confirm the structure.

Structure of OMe-AMD. The molecular structure of OMe-AMD determined by the X-ray diffraction method is shown in Figure 2. The overall structure of OMe-AMD is very similar to AMD structures found in the crystal structures of AMD itself[23] and DNA–AMD complexes.[12-14,34] The molecule possesses a pseudo-2-fold symmetry axis passing through the O5---N10 line. The amino group (N2) and quinoid oxygen (O3) of the phenoxazone ring and two methoxyphenyl groups of D-OMeTyr residues break the 2-fold symmetry. The two cyclic depsipeptides adopt a rectangular shape conformation as observed in all AMD structures. There are two inter-ring hydrogen bonds between the amide group (N–H) of the D-OMeTyr residue in one ring and the carbonyl oxygen (=O) of the D-OMeTyr residue in the other ring. These two symmetrical hydrogen bonds appear to play a role in reducing the mobility of the cyclic depsipeptides. The major difference between the two rings is found in the conformation angles of *N*-Cα-Cβ-Cγ in D-OMeTyr residues, which are (+)*gauche* in the α-ring and *trans* in the β-ring. The methoxybenzyl groups which are substituted with isopropyl groups of AMD are located on the side opposite to the DNA if the analogue binds to DNA as found in the X-ray analyses of the DNA–AMD complex structures.[14,34]

The molecular structure of OMe-AMD determined by this study shows clearly that modifications of the D-Val residues in the cyclic depsipeptides are not accompanied by any geometrical changes in the DNA binding side of the molecule. This suggests

Scheme 2. Synthesis of an AMD Analogue Containing D-Tyr in Place of D-Val

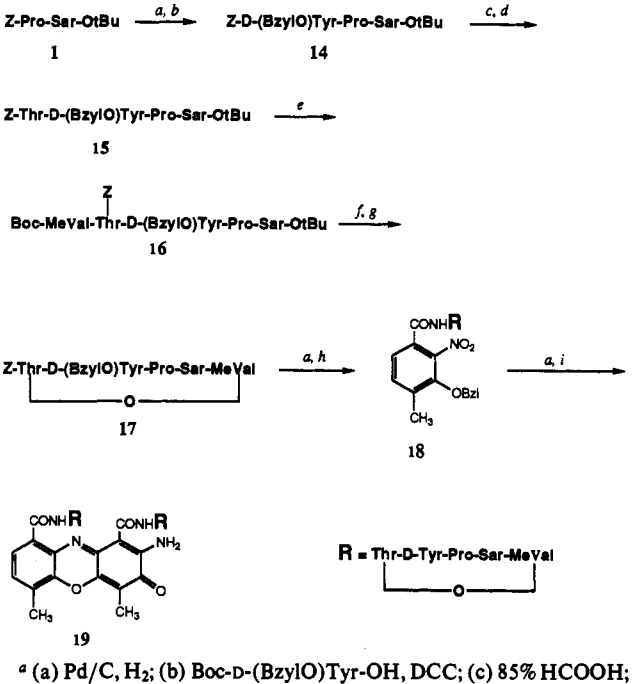

[a] (a) Pd/C, H_2; (b) Boc-D-(BzylO)Tyr-OH, DCC; (c) 85% HCOOH; (d) Z-Thr-OH, DCC; (e) Boc-MeVal, DCC, DMAP; (f) F_3CCOOH; (g) BOP-Cl, $N(Et)_3$; (h) BMNBCA, DCC; (i) $K_2Fe(CN)_6$, pH 7.12.

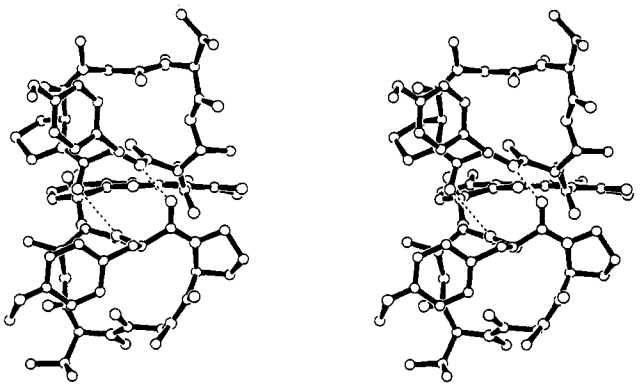

Figure 2. Molecular structure of OMe-AMD determined by the X-ray diffraction method. The inter-ring hydrogen bonds are drawn with dotted lines. The α- and β-rings of AMD referred to in the text are the cyclic depsipeptides located below and above the phenoxazone ring in the figure, respectively.

that the AMD analogue can bind intercalatively to DNA and the two threonine residues in the cyclic depsipeptides form four essential hydrogen bonds with the guanine ring of DNA as observed in the DNA–AMD complexes. A simple molecular modeling demonstrated that the AMD molecule in the complex of the d(GAAGCTTC)$_2$–AMD structure[34] was substituted with the OMe-AMD molecule determined by this study without any difficulty (Figure 3). As will be discussed later, however, the binding and biological characteristics of D-valine analogues are not the same as those of AMD itself in spite of the structural similarity described here.

As illustrated in Figure 4, two OMe-AMD molecules related by a crystallographic 2-fold symmetry constitute a dimer in the crystals as observed in the crystal structure of AMD itself.[23] The dimer is tightly connected together with three sets of symmetrical hydrogen bonds, which are the amino group (—N2) attached to the phenoxazone ring hydrogen-bonded to the carbonyl oxygen (=O17), the carbonyl oxygen (=O) of the threonine residue of the symmetry related molecule, and the quinoid oxygen (=O3) with the amide group (>NH) of the threonine residue. Furthermore the dimer is stabilized by a stacking interaction between

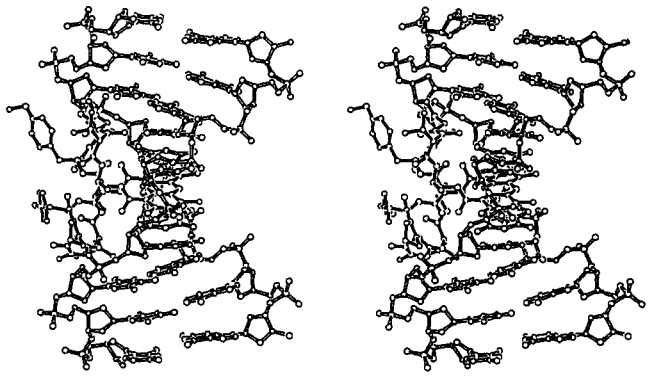

Figure 3. DNA–OMeTyr$_2$-AMD complex model derived from the crystal structure of d(GAAGCTTC)$_2$–AMD.[16] The phenoxazone ring of OMe-AMD is superimposed on the ring of AMD by the least-squares procedure. Neither the DNA nor the analogue's conformation was changed. There is no unusual short contact between DNA and the docked analogue. The DNA and the drug are drawn with open and solid bonds, respectively.

the two phenoxazone rings related by a 2-fold symmetry. The methoxyphenyl group in the α-ring is stacked on the phenoxazone ring of the neighboring dimer. These stacking interactions connect the dimers to form a three-dimensional network (Figure 5).

Water Solubilities of AMD Analogues. Solubilities of the analogues in water were determined, since this physical characteristic may play an important role in their binding and biological characteristics. As listed in Table 1, the solubilities of aromatic analogues are very low in comparison that of with AMD. Formation of the three-dimensional stacking network observed in the crystal structure of OMe-AMD probably reduces drastically the water solubility of the aromatic analogues. In the crystal structure of AMD itself,[23] three independent molecules are found. Two of them constitute a dimer as observed in this study, but the third stays as a monomer. There is no other stacking interaction between AMD dimers and/or monomers in the crystal, suggesting that the AMD dimer can easily dissociate to two monomers in an aqueous solution. Thus, when the two crystal structures of AMD and OMe-AMD are compared to each other, it is quite obvious why the water solubilities of AMD and the aromatic AMD analogues are very different from each other.

Surprisingly the water solubility of Thr-AMD is also quite small in comparison with that of AMD (31 vs 2900 μg/mL). It should be noted that the differences between Val-AMD (AMD itself) and Thr-AMD are very little [$-CH(CH_3)_2$ vs $-CH(OH)-CH_3$], and furthermore, the $-CH(OH)CH_3$ group is generally more hydrophilic than the $-CH(CH_3)_2$ group. The naturally occurring AMD analogue D-*allo*-isoleucine–actinomycin has been found to be more water soluble than AMD itself in spite of possessing a large hydrophobic group than AMD.[30] However, this study indicates that replacements of isopropyl groups with much larger hydrophobic groups such as benzyl and methoxybenzyl groups reduce drastically the water solubility of the analogues. As will be discussed later, the binding affinities of the AMD analogues are also reduced significantly. The binding of AMD is often described as being entropically driven in terms of the solvation of the free drug.[20,23,24] Therefore, if the hydration environments of the AMD analogues are quite similar to those of AMD, then our observation appears to be inconsistent with the previous studies on AMD.

DNA Binding Characteristics of AMD Analogues. It is important to examine whether there is any relationship between the transcription inhibitory activity and DNA binding characteristics of the AMD analogues. If there is a strong correlation between binding and inhibition, that would suggest that the transcription inhibitory activity of AMD is mainly due to its strength of DNA binding. On the other hand, if there is no clear relationship between binding and inhibitory activity, then the transcription inhibitory activity of AMD is not due only to its tight binding to DNA but also to other factors such as specific binding sites and unique structures of the cyclic depsipeptides.[35] Thus it is important to determine the DNA binding characteristics of AMD analogues in order to interpret the transcription inhibitory data. From the crystal structures of OMe-AMD, it is very clear that the chromophore of AMD cannot bind to the major and/or minor groove of DNA as do typical minor groove binding agents, such as netropsin and distamycin,[46] since there are not enough polar groups (–NH, –OH, >N, =O, and >O) on the surface of the chromophore. Therefore, the possible binding mode of the AMD analogues is either intercalation or weak side binding to the charged phosphate backbone of DNA. Since the visible spectrum (350–600 nm) of the chromophore is slightly shifted to the longer wavelength region (red shift) and the magnitudes of absorbance by the drug intercalating into the nucleic acid are reduced (hypochromic effect), the difference spectrum between the drug itself and the drug–DNA complex should resemble a negative sine curve if the drug binds intercalatively to oligonucleotides. Self-complementary oligonucleotides d(GAAGCTTC)$_2$ and d(GTTGCAAC)$_2$ with the drug binding site 5′-GC-3′ in the middle, poly(dG-dC), poly(dA-dT), and calf thymus DNA's were utilized to examine the binding characteristics of AMD and AMD analogues. The visible and corresponding difference spectra were measured at several different DNA:drug ratios in order to estimate the association constants of drugs.

It is noted that the buffer used for the binding study is a relatively low salt condition. We selected the buffer conditions to be as close as possible to the buffer conditions used in the inhibition of RNA synthesis, in order to eliminate the effects of different buffers on both experiments so we could compare easily the results of the binding study with the results of the RNA inhibition study. Although the binding experiment was carried out at a relatively low concentration of drugs (1 μM) in order to eliminate any possibility of dimerization of the drug in an aqueous solution, the possibility of dimerization in the buffer solution used in this study was examined by measuring the absorbance of 440 nm at various temperatures (20, 30, 40, 50, 60, 70, and 80 °C). No significant change in the absorbance was observed, suggesting that neither AMD nor AMD analogues formed detectable amounts of dimers at 1 μM concentration. It should be noted that the dimerization equilibrium constant of AMD was reported to be 2.7×10^3 M^{-1}, determined by the NMR method.[47] Using this dimerization equilibrium constant, 99.7% of AMD molecules are calculated to be dissociated from the dimers at 1 μM concentration. The dimerization equilibrium constants of the AMD analogues might be slightly larger than the value of AMD, since the crystal structure of OMe-AMD indicated that the molecules formed the stable dimers in solids. For this reason, even if the dimerization equilibrium constants of AMD analogues (2.7×10^5) are estimated 2 orders higher than the value for AMD, the equilibrium calculation indicates that 81.9% of the molecules are still dissociated from the dimers at 1 μM concentration.

Difference spectra of AMD and AMD analogues with d(GAAGCTTC)$_2$ and d(GTTGCAAC)$_2$ are given in Figures 6 and 7, respectively. All AMD analogues show significant difference spectra, suggesting that the analogues bind intercalatively to oligonucleotides. However, the difference spectra of AMD and the analogues are significantly different from each other. Furthermore, the difference spectra of the same analogue but with different oligonucleotides are also significantly different from each other, suggesting that an individual drug has some binding sequence preference. AMD shows the most significant difference spectra whereas the aromatic analogues give the smallest spectra, suggesting that AMD binds to oligonucleotides more strongly than do the aromatic analogues. The spectra of Thr-AMD are intermediate between those of AMD and aromatic AMD analogues. It should be noted that the X-ray and molecular modeling studies indicate that modification of the D-valine residues of AMD does not affect the conformation of the molecule and

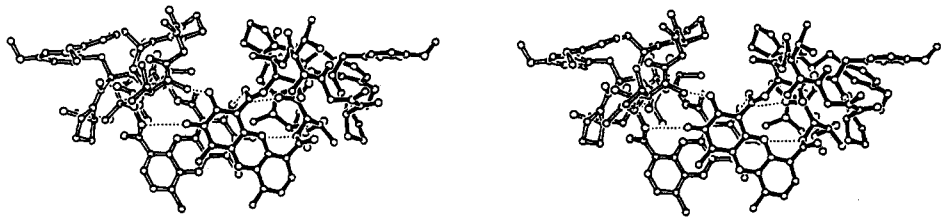

Figure 4. Structure of a tight dimer found in the crystal structure of OMe-AMD. The two molecules are drawn with solid bonds and open bonds, respectively, which are related to each other by a 2-fold symmetry. Hydrogen bonds are drawn with dotted lines.

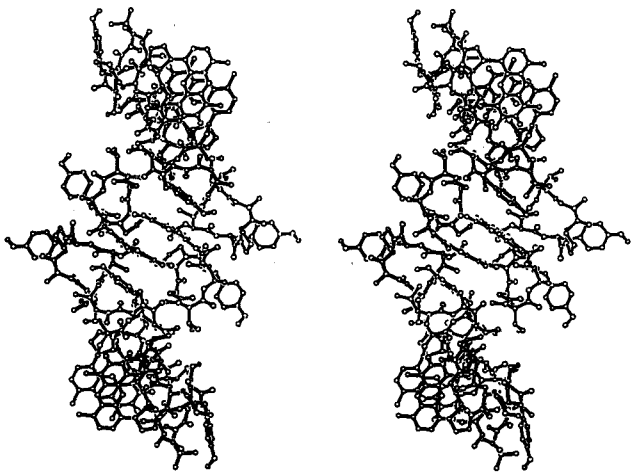

Figure 5. Molecular packing diagram viewed along a 2-fold axis showing that a pair of phenoxazone rings is further sandwiched by two methoxyphenyl groups of neighboring molecules. The molecules drawn with solid and open bonds form tight dimers.

Table 1. Solubility of AMD and AMD Analogues in Aqueous Solution at 22 ± 1 °C

drug	solubility (μg/mL)	drug	solubility (μg/mL)
AMD	2900	Phe-AMD	2.6
Thr-AMD	31	OMe-AMD	1.8
Tyr-AMD	3.7		

newly substituted groups of the analogues appear not to be involved in the interaction with DNA. However, replacements of D-valines with aromatic residues do affect on the DNA binding characteristics.

The association constants, *K*'s, were obtained by using eq 3 described below[37] and are listed in Table 2. Although AMD analogues were expected to bind intercalatively to the oligonucleotides as strongly as AMD itself, this study shows that the association constants of the aromatic analogues are approximate one-half that of AMD. The association constants with d(GTTGCAAC)$_2$ are significantly higher than those with d(GAAGCTTC)$_2$, especially for AMD and Thr-AMD for which the ratios of the association constants are more than 4.0. Our observations are quite consistent with the AMD binding order of TGCA > CGCG > AGCT ≫ GGCC, which was determined by using a series of self-complementary decamers of the sequence d(ATAXGCYTAT)$_2$.[28] The other recent kinetic study on AMD–DNA interactions also shows that the association constant of AMD with the oligonucleotide with a 5′-TGCA-3′ binding sequence is the highest (4.0×10^6 M^{-1}) among the sequences TGCA, CGCA, and TCGT.[18]

The visible spectra of AMD and OMe-AMD measured at various concentrations of calf thymus DNA are shown in Figures 8 and 9, respectively. Since the spectra of other aromatic analogues Phe-AMD and Tyr-AMD were quite similar to that of OMe-AMD, the spectra of AMD and OMe-AMD are mainly compared hereafter. The AMD spectra showed significant red shifts and hypochromic effects when the DNA was added into the drug solution, suggesting that the drug intercalates to the

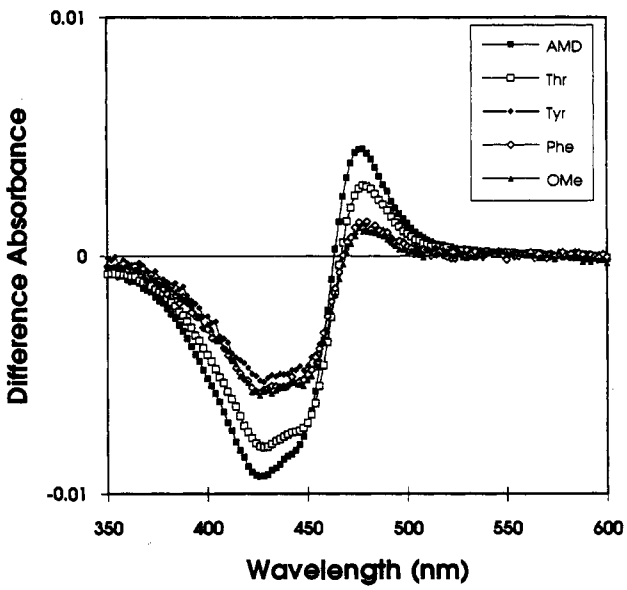

Figure 6. Difference spectra of AMD and AMD analogues with d(GAAGCTTC)$_2$. Concentrations of the drug and DNA are 1.0 and 2.0 μM, respectively, except for AMD and Thr-AMD whose drug:DNA ratios are 1:1.

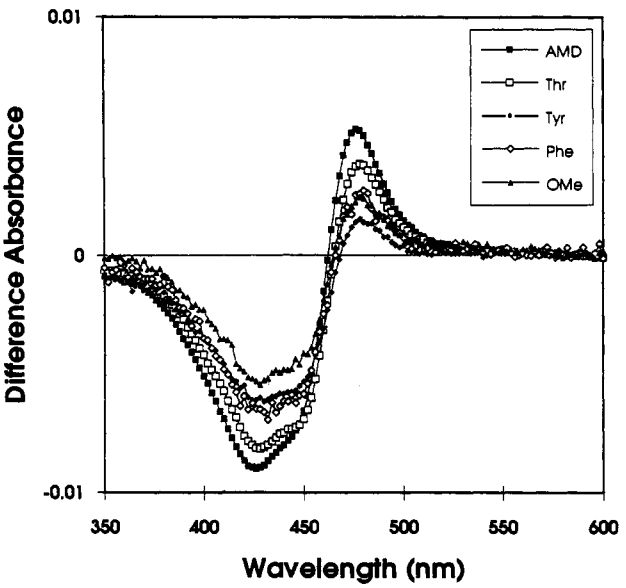

Figure 7. Difference spectra of AMD and AMD analogues with d(GTTGCAAC)$_2$. Concentrations of the drug and DNA are 1.0 and 2.0 μM, respectively, except for AMD and Thr-AMD whose drug:DNA ratios are 1:1.

DNA. A similar spectrum shift and hypochromic effect were observed with the Thr-AMD analogue. On the other hand, the spectra of the aromatic AMD analogues titrated with calf thymus DNA were somewhat different from those of AMD itself. As shown in Figure 9, the visible spectra of OMe-AMD showed only a little red shift upon increasing the DNA concentration though significant hypochromic effects were observed. Similar spectra were observed as shown in Figure 10 when AMD or OMe-AMD

Table 2. Association Constants (K, M^{-1}), Hypochromic Effect (H), and Red Shift ($\Delta\lambda$, nm) of AMD and AMD Analogues with Two Oligonucleotides[a]

	d(GAAGCTTC)$_2$			d(GTTGCAAC)$_2$			
drug	K_1	H	$\Delta\lambda$	K_2	H	$\Delta\lambda$	K_2/K_1
AMD	$1.1(2) \times 10^6$	0.56	23	$5.7(19) \times 10^6$	0.56	20	5.2
Thr-AMD	$5.3(4) \times 10^5$	0.58	19	$2.2(2) \times 10^6$	0.62	19	4.2
Tyr-AMD	$3.7(6) \times 10^5$	0.42	18	$6.6(1) \times 10^5$	0.52	17	1.8
Phe-AMD	$4.9(3) \times 10^5$	0.39	18	$8.5(6) \times 10^5$	0.48	17	1.7
OMe-AMD	$3.4(3) \times 10^5$	0.42	17	$5.6(6) \times 10^5$	0.51	16	1.6

[a] The root-mean-square (rms) deviations of the association constants are in parentheses.

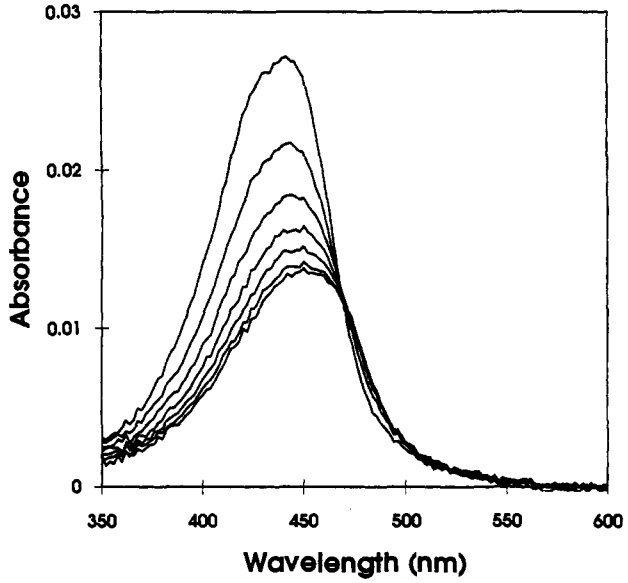

Figure 8. Visible spectra of AMD titrated by calf thymus DNA. The drug concentration is 1.1 μM. The spectra with ratios of base pairs per drug of 0, 5, 10, 15, 20, 25, and 30 are drawn from top to bottom, respectively.

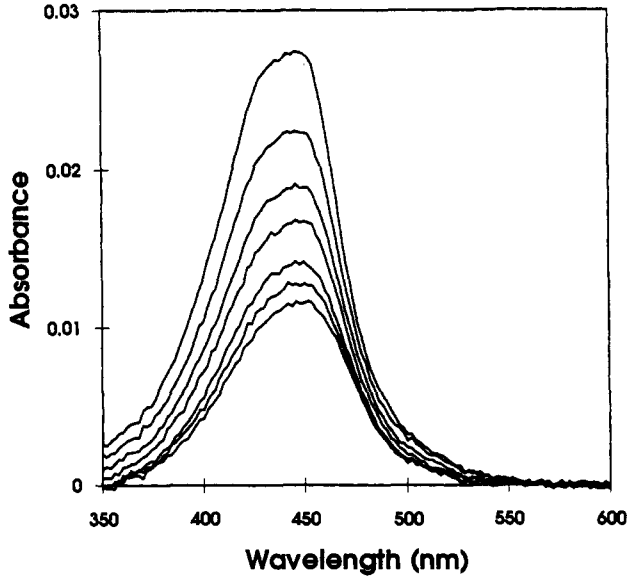

Figure 9. Visible spectra of OMe-AMD titrated by calf thymus DNA. The drug concentration is 1.0 μM. The spectra with ratios of base pairs per drug of 0, 5, 10, 15, 20, 25, and 30 are drawn from top to bottom, respectively.

was titrated with poly(dA-dT). In these cases, neither AMD nor OMe-AMD binds intercalatively to poly(dA-dT) since there is no binding sequence, 5′-GC-3′, in poly(dA-dT). It should be noted that the spectra of AMD titrated with NaCl were reminiscent of the spectra of AMD titrated with poly(dA-dT), showing no red shift but significant hypochromic effects.

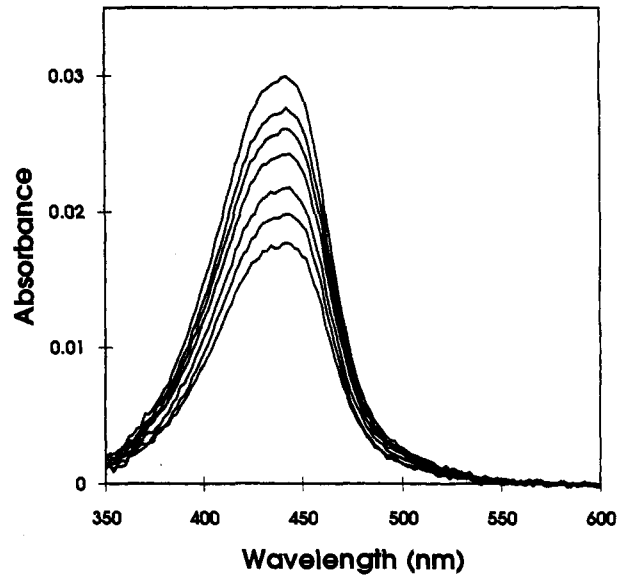

Figure 10. Visible spectra of AMD titrated by poly(dA-dT). The drug concentration is 1.0 μM. The spectra with ratios of base pairs per drug of 0, 5, 10, 15, 20, 25, and 30 are drawn from top to bottom, respectively.

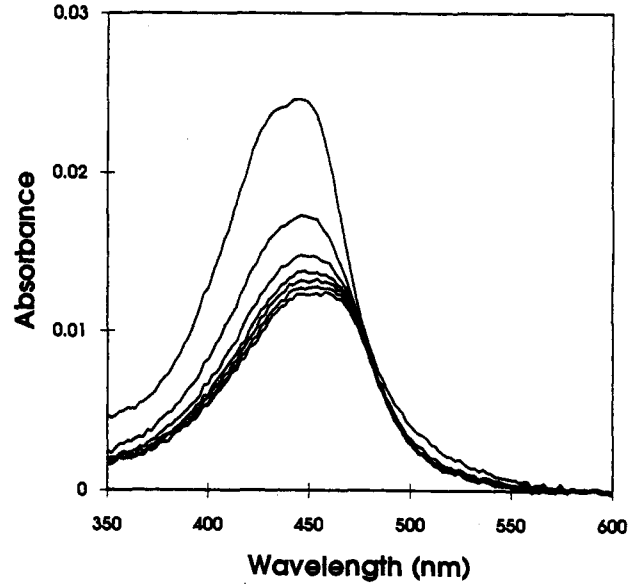

Figure 11. Visible spectra of OMe-AMD titrated by poly(dG-dC). The drug concentration is 1.0 μM. The spectra with ratios of base pairs per drug of 0, 5, 10, 15, 20, 25, and 30 are drawn from top to bottom, respectively.

Therefore, the interaction between AMD and poly(dA-dT) appears to be a side binding which is neither an intercalation nor a groove binding. Similar spectral changes have been reported when chromophores bind to DNA but do not intercalate into DNA.[38] As shown in Figure 11, the spectra of OMe-AMD titrated with poly(dG-dC) show clear red shifts as well as hypochromic effects, but the spectra of complexed drugs do not cross over the spectrum of the free drug at the longer wavelength region, indicating that the typical small shoulders observed in difference spectra (Figures 6 and 7) do not appear in the difference spectra of the aromatic AMD analogues. These spectral data indicate that the mode of binding of aromatic AMD analogues to the long DNA's (calf thymus DNA and poly(dG-dC)) is somehow different from the mode of binding to the short oligonucleotides.

A simple least-squares technique has been developed in order to analyze quantitatively the spectra described above. In general, when a drug intercalates into DNA, the visible spectrum of the

(38) Kuroda, R.; Takahashi, E.; Austin, C. A.; Fisher, L. M. *FEBS Lett.* **1990**, *262*, 293–298.

drug is slightly shifted to the longer wavelength region by $\Delta\lambda$ and the magnitude of absorbance is reduced by the hypochromic effect. The shape of the visible spectrum of the complexed drug is quite similar to the spectrum of the free drug. Thus, a spectrum of a drug–DNA solution which contains spectra of the free drug and the complexed drug can be represented as the sum of the two relatively weighted observed spectra of the free drug, in which one of the spectra is shifted by $\Delta\lambda$. The calculated absorbance of the drug–DNA complex at wavelength λ, $A_c(\lambda)_{calcd}$, can be represented as the sum of the observed absorbances of the free drug at λ and $\lambda - \Delta\lambda$:

$$A_c(\lambda)_{calcd} = C_0 A_d(\lambda)_{obsd} + C_1 A_d(\lambda - \Delta\lambda)_{obsd} \qquad (1)$$

where $A_d(\lambda)_{obs}$ and $A_d(\lambda-\Delta\lambda)_{obs}$ are the observed absorbances of the free drug at the wavelengths of λ and $\lambda - \Delta\lambda$. The coefficients C_0 and C_1 and the shift parameter $\Delta\lambda$ can be determined by minimizing $\sum(A_c(\lambda)_{obsd} - A_c(\lambda)_{calcd})^2$. The discrepancy factor R is used to judge agreement between the observed and calculated spectra:

$$R = \sum|A_c(\lambda)_{obsd} - A_c(\lambda)_{calcd}|/\sum|A_c(\lambda)_{obsd}|$$

If the spectra contain a significant red shift component, then the coefficient C_1 and the $\Delta\lambda$ will be significant positive quantities. The coefficient C_1 is the product of the ratio of the intercalated drug (α) and its hypochromic effect (H), *i.e* $C_1 = \alpha H$. The association constant K is defined as

$$K = \alpha/[(1-\alpha)(E-\alpha)D]$$

$$= (C_1/H)/[(1-(C_1/H))(E-(C_1/H))D] \qquad (2)$$

where the D and E are the total concentration of the drug and the ratio of DNA (in units of bp) per drug, respectively. Under conditions in which the hypochromic effect (H) and the association constant (K) are constant for any drug concentration (D) and ratio of DNA per drug (E), the best α and H can be determined by minimizing $\sum(K_i - K_j)^2$, where K_i and K_j are the association constants calculated from the different ratios of DNA:drug.

If the visible absorbance spectra of the drug with calf thymus DNA are changed only by intercalation of drugs, then the coefficient C_0 should be $1 - \alpha$. Thus, the ratio of intercalation (α), hypochromic effect (H), and association constant (K) are defined as

$$\alpha = 1 - C_0 \qquad H = C_1/\alpha$$

$$K = \alpha/[(1-\alpha)(E-\alpha)D] = (1-C_0)/[C_0(E + C_0 - 1)D] \qquad (3)$$

The association constants obtained from the coefficient C_0 using eq 3 should agree with those determined from the coefficient C_1 using eq 2, if the assumption described above is valid. On the other hand, if the spectra are changed not only by an intercalation effect but also by side-binding effects, then the coefficient C_0 would contain the side-binding effect since in general the side binding changes a magnitude of absorbance (hypochromic effect) but does not accompany a red shift of the spectrum. If this is the case, the coefficient C_0 can be represented as $C_0 = (1 - \alpha - X)$, where X is an overall effect caused by the side binding of drugs. Therefore if drugs bind to DNA with both intercalation and side-binding modes, the association constant K determined from eq 3 is always larger than the association constant K calculated from eq 2. The overall effect (X) caused by the side binding on the spectra cannot be characterized simply since the side binding might contain many different binding modes, such as interaction with phosphate groups, interaction with bases, interaction with sugars, and interaction with drugs already bound to DNA.

Table 3. Summary of Spectral Analyses of AMD and AMD Analogues Titrated with Calf Thymus DNA and Poly(dG-dC)[a]

drug	calculated from C_0 and eq 3		calculated from C_1 and eq 2		
	H	K	H	K	$\Delta\lambda$
(1) Spectra Titrated with Calf Thymus DNA					
AMD	0.42	$1.3(2) \times 10^5$	0.45	$1.0(1) \times 10^5$	19
Thr-AMD	0.38	$9.4(10) \times 10^4$	0.40	$8.3(6) \times 10^4$	18
Tyr-AMD	0.25	$6.8(13) \times 10^4$	0.50	$1.9(1) \times 10^4$	10
Phe-AMD	0.30	$5.0(10) \times 10^4$	0.37	$3.3(3) \times 10^4$	14
OMe-AMD	0.24	$6.1(9) \times 10^4$	0.23	$6.6(12) \times 10^4$	9
(2) Spectra Titrated with Poly(dG-dC)					
AMD	0.47	$6.5(18) \times 10^5$	0.44	$1.1(4) \times 10^6$	23
Thr-AMD	0.52	$5.0(8) \times 10^5$	0.48	$7.7(3) \times 10^5$	20
Tyr-AMD	0.45	$2.2(2) \times 10^5$	0.41	$3.8(2) \times 10^5$	16
Phe-AMD	0.50	$2.3(4) \times 10^5$	0.44	$4.7(7) \times 10^5$	18
OMe-AMD	0.45	$1.9(3) \times 10^5$	0.40	$3.5(4) \times 10^5$	15

[a] Hypochromic effects (H) and association constants (K, bp M^{-1}) were determined from the coefficients C_0 and C_1 using eqs 2 and 3, respectively. The red shifts ($\Delta\lambda$, nm) of the spectra were obtained by using eq 1. The rms deviations of the association constants are in parentheses.

Using the procedures described above, the spectra of AMD and aromatic AMD analogues were analyzed, and the results are summarized in Table 3. The discrepancy factors (R), of all spectra are less than 0.04, suggesting that eq 1 is an acceptable approximation. The red shift components (C_1) of the AMD and OMe-AMD spectra titrated with poly(dA-dT) are zero even though the concentration of DNA is very high (50 bp/molecule of drug), indicating that neither AMD nor OMe-AMD intercalate into poly(dA-dT). The reduction of absorbance of the chromophore upon titrating with poly(dA-dT) is due to a side-binding effect. Although the spectra of OMe-AMD titrated with calf thymus DNA appear to be quite similar to those of AMD titrated with poly(dA-dT), the red shift components (C_1) of the titration with calf thymus DNA are significantly positive quantities, indicating that OMe-AMD does intercalate into calf thymus DNA. However, the mean red shifts ($\Delta\lambda$) of AMD and OMe-AMD were found to be quite different from each other (19.0 ± 1.0 nm for AMD and 9.0 ± 1.5 nm for OMe-AMD). The hypochromic effects (H) were also different from each other (0.42 for AMD and 0.24 for OMe-AMD). Although the association constants (K) and hypochromic effects (H) of AMD and AMD analogues determined by the two independent methods agree reasonably well with each other, a systematic difference is observed in the pair of association constants. The association constant (1.3×10^5 bp M^{-1}) of AMD calculated from the coefficient C_0 using eq 3 is slightly larger than that calculated from the coefficient C_1 using eq 2 (1.0×10^5 bp M^{-1}), indicating that the major binding mode of AMD is intercalation but a small portion involves side binding. As listed in Table 3, the same trend is observed in the association constants of AMD analogues. It is difficult to determine what percentage of molecules is involved in side binding, since the side binding contains multiple binding modes as described above. The association constants of the aromatic AMD analogues are approximately one-half that of AMD. Similar reductions in the association constants are observed in the cases of the short oligonucleotides (Table 2). The association constants to poly(dG-dC) are also given in Table 3. In all compounds, the association constants determined from the coefficient C_1 are larger than those determined from the coefficient C_0, suggesting that the major mode of binding of AMD and the AMD analogues to poly(dG-dC) is intercalation.

The melting profiles of calf thymus DNA and poly(dA-dT) with and without drugs were measured in order to examine whether sufficient amounts of the aromatic AMD analogues bind intercalatively to calf thymus DNA. The DNA structure is further stabilized by the drug intercalation, and consequently, the melting point of DNA is increased. On the other hand, a side binding

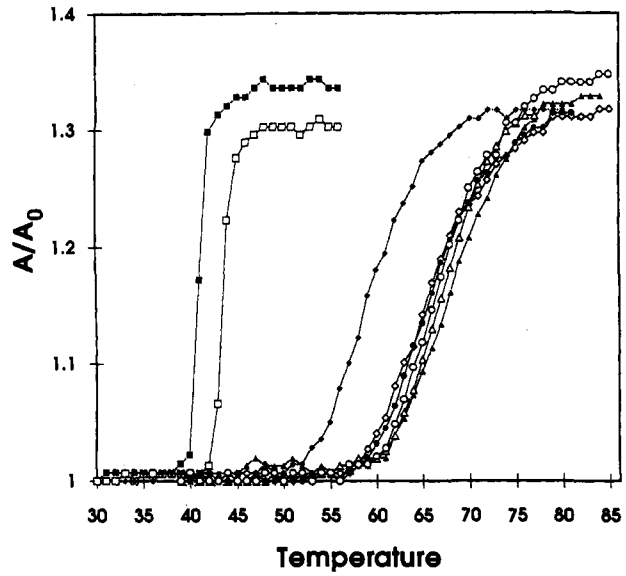

Figure 12. Melting profiles of poly(dA-dT) and calf thymus DNA with and without AMD and AMD analogues. The concentration of DNA is 10 bp/molecule of drug at a drug concentration of 1.0 μM. The melting profiles of poly(dA-dT) itself (■) and poly(dA-dT) with AMD (□) are illustrated in the left side of the figure, while the melting profiles of calf thymus itself (◆) with AMD (◇), Thr-AMD (▲), Tyr-AMD (△), Phe-AMD (●), and OMe-AMD (○) are shown in the right side of the figure.

requires only a few weak interactions between the drug and DNA, and thus, the drugs dissociate from DNA rapidly upon increasing temperature. As a result, the melting point of DNA is changed little by side bindings of drugs. The DNA melting profiles of calf thymus DNA and poly(dA-dT) were measured with drugs (10 bp/molecule of drug) and without drugs by monitoring the absorbance at 260 nm. The melting profiles of noncomplexed and complexed DNA's are shown in Figure 12. The melting point of calf thymus DNA is increased by approximately 10 °C when AMD molecules bind to the DNA, whereas the melting point is increased by only a few degrees when AMD molecules bind to poly(dA-dT). These differences in melting behaviors between calf thymus DNA and poly(dA-dT) are quite consistent with the fact that AMD binds intercalatively to calf thymus DNA while AMD cannot intercalate to poly(dA-dT) but binds with side-binding mode. It should be noted that the melting profiles of poly(dA-dT) at different DNA:AMD ratios (5 and 2.5 bp/molecule of AMD) were superimposable on the profile recorded at the ratio of 10 bp/molecule of AMD, suggesting that side binding (which is neither intercalation nor groove binding) does not stabilize the DNA structure as much as intercalation does. As shown in Figure 12, the melting curves of calf thymus DNA with the aromatic AMD analogues are all superimposable on that of the same DNA with AMD within experimental error, suggesting that all AMD analogues stabilize the DNA structure by binding intercalatively to the DNA as AMD does. These DNA melting behaviors support the results of the visible spectrum analysis, in which the aromatic AMD analogues intercalate into calf thymus DNA as AMD does, although the titration spectra appear to be quite different from those of AMD.

It should be noted that the spectra of both AMD and OMe-AMD titrated with short oligonucleotides showed large red shifts ($\Delta\lambda$ = 16–23 nm). The spectra of AMD titrated with calf thymus DNA and poly(dG-dC) also show the same magnitude of red shift ($\Delta\lambda$ = 19–23 nm), suggesting that AMD intercalates into both short oligonucleotides and long DNA's in a quite similar fashion. On the other hand, the spectra of the aromatic AMD analogues titrated with calf thymus DNA and poly(dG-dC) show relatively small red shifts ($\Delta\lambda$ = 9 and 18 nm), indicating that the analogues bind to the long DNA's somehow differently than to the short oligonucleotides. Recent crystal structure analysis of DNA–AMD complexes revealed that AMD has multiple

Table 4. Drug Concentration at 50% Inhibition of RNA Synthesis

drug	concn (μg/mL)	drug	concn (μg/mL)
AMD	0.40	Phe-AMD	0.22
Thr-AMD	0.53	OMe-AMD	1.90
Tyr-AMD	0.85		

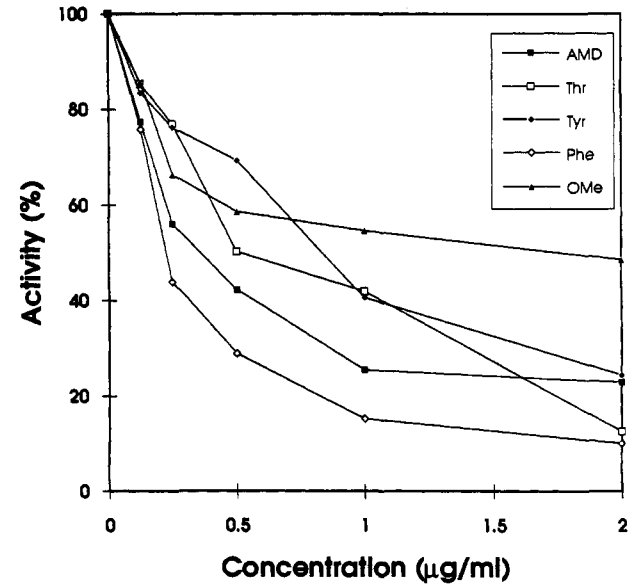

Figure 13. Inhibition profiles of AMD and AMD analogues.

intercalation modes.[34] In the complex structures, the guanine rings stack dominantly with the chromophore in some cases and both guanine and cytosine rings stack equally with the chromophore in other cases. If one of the stacking patterns found in the DNA–AMD complexes is localized in the OMe-AMD complex and/or the base pairs stack completely differently on the chromophore of OMe-AMD from the way they do on that of AMD, then the red shift of its spectrum may differ from that of AMD. Another possibility is that the analogues intercalate preferentially into different sequence sites, such as 5′-GT-3′.[18] Also we cannot completely eliminate the possibility of the influence of substituted aromatic groups on the chromophore spectra, though no significant differences in the red shifts were observed between the spectra of AMD and the aromatic AMD analogues titrated with oligonucleotides. A further investigation is necessary to determine what factors control the modes of binding of the aromatic AMD analogues to the long DNA's.

Inhibition of RNA Synthesis. AMD and AMD analogues were examined for their ability to inhibit RNA synthesis *in vitro* using calf thymus DNA and *E. coli* RNA polymerase. The drug concentrations at 50% inhibition of RNA synthesis (I_{50} in μg/mL) are listed in Table 4, and the inhibition profiles are shown in Figure 13. All AMD analogues severely inhibit RNA synthesis at relatively low drug concentrations. However, there are significant variations among the drug concentrations at 50% inhibition of RNA synthesis. In general, tighter-binding analogues tend to inhibit RNA synthesis better, except for Phe-AMD. The Phe-AMD analogue inhibits RNA synthesis more strongly than AMD itself, but the analogue binds to the oligonucleotides and calf thymus DNA much more weakly than AMD. If RNA synthesis inhibitory activity of the analogue is due to binding to DNA, the phenyl groups of the analogue must somehow participate in interrupting polymerase activity when the polymerase reaches drug binding sites. Another possibility is that Phe-AMD binds not only to DNA but also to RNA polymerase, and this causes additional inhibition of RNA polymerase activity. Unfortunately this study cannot distinguish between these two possibilities. It is noted that, as described by Müller and Crothers,[11] if Phe-AMD dissociates from the DNA relatively slowly, then the Phe-AMD analogue becomes a strong inhibitor yet a relatively weak binder. Although Brockmann *et*

al.[36] reported that D-Ala_2-AMD and D-Leu_2-AMD analogues were biologically inactive, our D-valine analogues have an inhibitory activity on RNA synthesis at least *in vitro*.

Conclusion

The X-ray structure of OMe-AMD indicated that replacement of D-valine residues with other D-amino acid residues did not change the overall conformation of the cyclic depsipeptides. A simple molecular modeling study suggested that the OMe-AMD molecule can intercalate into $d(GAAGCTTC)_2$ in exactly the same fashion as observed in the crystal structures of $d(GAAGCTTC)_2$–AMD complexes. The replaced groups were located on the side opposite to the DNA binding site, suggesting there should be no effect on the DNA binding capacity.

However, the difference spectra of the aromatic AMD analogues with $d(GAAGCTTC)_2$ and $d(GTTGCAAC)_2$ were not exactly the same as those of AMD, indicating replacement of the D-valine residues with the aromatic residues does affect the binding capacities of the analogues. As a result of replacement of the D-valine residues, the association constants of the analogues with DNA were reduced approximately to one-half that of AMD. The effects of replacement of the D-valine residues were further amplified in the binding characteristics with calf thymus DNA. The aromatic analogues bound the DNA not only with intercalation but also with the side binding. However, the DNA melting profile analyses at the concentration of 10 bp/molecule of drug indicated that enough analogue molecules intercalated into the DNA to stabilize the structure of DNA as AMD does.

As observed in the binding characteristics, replacement of D-valine residues with the aromatic amino acid residues affected the ability of the drug to inhibit RNA synthesis *in vitro*. In general, tighter-binding analogues tend to inhibit RNA synthesis better, except for Phe-AMD. The Phe-AMD analogues inhibited RNA synthesis more strongly than AMD itself, but the analogue bound to the oligonucleotides and calf thymus DNA much more weakly than does AMD.

Although the D-valine residue in the cyclic depsipeptide of AMD is not involved directly in binding to DNA, this amino acid residue appears to be an important biological modulator of AMD. The D-valine residues play an important role in increasing the water solubility of the antibiotic. Replacements of the D-valine residues reduced drastically the water solubility of the analogues, and consequently, this physical characteristic of the analogues reduced their capacities for binding to DNA. As a result, the biological activities of the analogues were generally decreased. However, the exception is that the D-phenylalanine analogue has now been found to have unusually strong RNA synthesis inhibitory activity.

Experimental Section

Syntheses. Melting points are uncorrected. The NMR spectra were obtained with a 300-MHz Varian XL-300 NMR spectrometer. For the mass spectrum measurements, electron ionization (EI) and chemical ionization (CI) spectra were obtained on a Nermag R10-10 quadrupole GC/MS system with a SPECTRAL 30 data system. Fast-atom bombardment mass spectra (FABMS) were obtained on a ZAB HS mass spectrometer. All mass spectrum measurements have been carried out at the Mass Spectrometry Laboratory of the University of Kansas under director T. D. Williams. The homogeneity of the products was checked by thin-layer chromatography on silica gel plates. Abbreviations used are BOP-Cl = *N,N*-bis(2-oxo-3-oxazolidinyl)phosphorodiamidic chloride, DCC = dicyclohexylcarbodiimide, DCM = dichloromethane, and DMAP = 4-(*N,N*-dimethylamino)pyridine.

***N*-(Benzyloxycarbonyl)prolylsarcosine *tert*-Butyl Ester (1).** A solution of (benzyloxycarbonyl)sarcosine *tert*-butyl ester (4.82 g, 17.3 mM) in methanol (30 mL) was hydrogenated over 10% Pd/C (0.56 g) at atmospheric pressure for 2 h with stirring. After filtration the filtrate was evaporated *in vacuo*. To a solution of the residue and (benzyloxycarbonyl)proline (4.30 g, 17.3 mM) in DCM (40 mL) was added a solution of DCC (3.56 g, 17.3 mM) in DCM (10 ml) at −10 °C. The reaction mixture was stirred for 3 h at −10 °C and then kept overnight in a refrigerator. After removal of *N,N'*-dicyclohexylurea (DCurea) by filtration, the filtrate was evaporated *in vacuo*. The residue was dissolved in ethyl acetate (80 mL), and the solution was washed with 10% citric acid (2 × 15 mL), 1 M $NaHCO_3$ (2 × 15 mL), and water (20 mL) and dried over anhydrous Na_2SO_4. After evaporation of the ethyl acetate *in vacuo*, the residue was purified by the flash column chromatography on silica gel with ethyl acetate–hexane (1:2) to afford 5.65 g (87%) of **1** as a colorless liquid: $[\alpha]^{23}_D$ −57.4° (*c* 1.0, MeOH); CIMS in NH_3 *m/z* (relative intensity) 377 (M + 1, 100) indicated M = 376 ($C_{20}H_{28}N_2O_5$ requires M = 376.45); NMR ($CDCl_3$) δ 7.33 (s, Bzl ArH), 3.12 (s, NCH_3), 1.44 (s, OtBu).

***N*-(Benzyloxycarbonyl)-D-phenylalaninylprolylsarcosine *tert*-Butyl Ester (2).** A solution of **1** (3.78 g, 0.01 mol) in methanol (35 mL) was hydrogenated over 10% Pd/C (600 mg) at atmospheric pressure for 2 h with stirring. After filtration the filtrate was evaporated *in vacuo*. To a solution of residue and (benzyloxycarbonyl)-D-phenylalanine (2.99 g, 0.01 mol) in DCM (35 mL) was added a solution of DCC (3.1 g, 0.015 mol) in DCM (10 mL) at −10 °C. The reaction mixture was stirred for 3 h at −10 °C and then kept overnight in a refrigerator. After removal of DCurea by filtration, the filtrate was evaporated *in vacuo*. The residue was dissolved in ethyl acetate (100 mL), and the solution was washed with 10% citric acid (2 × 15 mL), 1 M $NaHCO_3$ (2 × 15 mL), and water (2 × 15 mL) and dried over anhydrous Na_2SO_4. After evaporation of the ethyl acetate *in vacuo*, the residue was purified by the flash column chromatography on silica gel with hexane–ethyl acetate (1:1) to afford 4.47 g (85%) of **2** as a colorless liquid: $[\alpha]^{23}_D$ −53.9° (*c* 2.0, MeOH); NMR ($CDCl_3$) δ 7.33 (s, Bzl ArH), 7.25 (s, Phe ArH), 3.12 (s, NCH_3), 1.43 (s, OtBu); FABMS *m/z* (relative intensity) 524 (M + H, 40); HRMS calcd for $C_{29}H_{37}N_3O_6$ (M + H) 524.2761, found 524.2787.

***N*-(Benzyloxycarbonyl)threonyl-D-phenylalaninylprolylsarcosine *tert*-Butyl Ester (3).** A solution of **2** (2.50 g, 4.78 mM) in methanol (25 mL) was hydrogenated over 10% Pd/C (300 mg) at atomospheric pressure for 2 h with stirring. After filtration the filtrate was evaporated *in vacuo*. To a solution of the residue and (benzyloxycarbonyl)threonine (1.21 g, 4.78 mM) in DCM (20 mL) was added a solution of DCC (0.98 g, 4.76 mM) in dichloromethane (5 mL) at −10 °C. The reaction mixture was stirred for 3 h at −10 °C and kept overnight in a refrigerator. After removal of DCurea by filteration, the filtrate was evaporated *in vacuo*. The residue was dissolved in ethyl acetate (70 mL), and the solution was washed with 10% citric acid (2 × 15 mL), 1 M $NaHCO_3$ (2 × 15 mL), and water (2 × 20 mL) and dried over anhydrous Na_2SO_4. After evaporation of the ethyl acetate *in vacuo*, the residue was purified by the flash column chromatography on silica gel with ethyl acetate to afford 2.12 g (71%) of **3** as a white amorphous solid: $[\alpha]^{23}_D$ −59.1° (*c* 1.0, MeOH); NMR ($CDCl_3$) δ 7.34 (s, Bzl ArH), 7.24 (s, Phe ArH), 3.09 (NCH_3), 1.43 (s, OtBu), 1.16 (Thr CH_3); FABMS *m/z* (relative intensity) 625 (M + H, 90); HRMS calcd for $C_{33}H_{44}N_4O_8$ (M + H) 625.3237, found 625.3262.

***O*-(*tert*-Butoxycarbonyl)-*N*-methylvalyl-*N*-(benzyloxycarbonyl)threonyl-D-phenylalaninylprolylsarcosine *tert*-Butyl Ester (4).** To a solution of **3** (2.00 g, 3.21 mM) and (*tert*-butoxycarbonyl)-*N*-methylvaline (0.96 g, 4.17 mM) in DCM (25 mL) were added DMAP (195 mg, 1.61 mM) and a solution of DCC (860 mg, 4.17 mM) in DCM (15 mL) at 0 °C. The reaction mixture was stirred for 2 h at 0 °C and 12 h at room temperature. After removal of DCurea by filtration, the filtrate was evaporated *in vacuo*. The residue was dissolved in ethyl acetate (100 mL), and the solution was washed with 10% citric acid (2 × 20 mL), 1 M $NaHCO_3$ (2 × 20 mL), and water (2 × 20 mL) and dried over anhydrous Na_2SO_4. After evaporation of the ethyl acetate *in vacuo*, the residue was purified by the flash column chromatography on silica gel with hexane–ethyl acetate (1:2) to afford 2.48 g (93%) of **4** as a white amorphous solid: $[\alpha]^{23}_D$ −61.5° (*c* 1.0, MeOH); NMR ($CDCl_3$) δ 7.35 (s, Bzl ArH), 7.24 (s, Phe ArH), 3.11 (s, NCH_3), 2.79 (s, NCH_3), 1.48 (s, OtBu), 1.43 (s, OtBu), 1.18 (d, Thr CH_3), 0.92 (d, MeVal CH_3), 0.87 (d, MeVal CH_3); FABMS *m/z* (relative intensity) 845 (M + Li, 100); HRMS calcd for $C_{44}H_{63}N_5O_1$ (M + H) 838.4602, found 838.4624.

***N*-(Benzyloxycarbonyl)threonyl-D-phenylalaninylprolylsarcosyl-*N*-methylvaline Lactone (5).** A solution of **4** (1.28 g, 1.53 mM) in trifluoroacetic acid (14 mL) was stirred at 0 °C for 4 h. After evaporation of the trifluoroacetic acid *in vacuo*, the residue was dissolved in ethyl acetate (100 mL), then evaporated *in vacuo*. Ethyl ether (150 mL) was added to the residue, and the solid was filtered to give a deprotected peptide salt with trifluoroacetic acid. To the solution of the solid in DCM (150 mL) was added triethylamine (348 mg, 3.44 mM) at 0 °C, and the mixture was diluted with DCM (600 mL) and BOP-Cl (586 mg, 2.3 mM) was added. The reaction mixture was stirred for 5 days at room temperature. After evaporation of the solution, the residue was dissolved in ethyl acetate

(100 mL) and the solid was separated by filtration. The filtrate was evaporated, and the residue was purified by the flash column chromatography on silica gel with ethyl acetate–methanol (10:1) to afford 638 mg (63%) of **5** as a colorless amorphous solid: $[\alpha]^{23}_D$ –54.6° (*c* 1.0, MeOH); NMR ($CDCl_3$) δ 7.4–7.2 (m, Bzl, Phe ArH), 3.31 (s, NCH_3), 3.14 (s, NCH_3), 1.23 (d, Thr CH_3), 0.89 (d, MeVal CH_3), 0.80 (d, MeVal CH_3); FABMS *m/z* (relative intensity) 664 (M + H, 100), 686 (M + Na, 40); HRMS calcd for $C_{35}H_{45}N_5O_8$ (M + H) 664.3346, found 664.3344.

(3-(Benzyloxy)-4-methyl-2-nitrobenzoyl)threonyl-D-phenylalaninylprolylsarcosyl-*N*-methylvaline Lactone (6). A solution of **5** (0.200 g, 0.30 mM) in methanol (15 mL) was hydrogenated over 10% Pd/C (0.15 g) at atmospheric pressure for 2 h with stirring. After filtration, the filtrate was evaporated *in vacuo*. To a solution of the residue and 3-(benzyloxy)-4-methyl-2-nitrobenzoic acid (86.6 mg, 0.30 mM) in DCM (8 mL) was added a solution of DCC (61.8 mg, 0.30 mM) in DCM (2 mL) at –10 °C. The reaction mixture was stirred for 3 h at –10 °C and then kept overnight in a refrigerator. After removal of DCurea by filtration, the solution was evaporated *in vacuo*. The residue was dissolved in ethyl acetate (100 mL), and the solution was washed with 10% citric acid (2 × 25 mL), 1 M $NaHCO_3$ (2 × 25 mL), and water (20 mL) and dried over anhydrous Na_2SO_4. After evaporation of the ethyl acetate *in vacuo*, the residue was purified by flash column chromatography on silica gel with ethyl acetate–methanol (10:1) to afford 0.172 g (72%) of **6** as a colorless solid: $[\alpha]^{23}_D$ +11.0° (*c* 0.6, CH_2Cl_2); NMR ($CDCl_3$) δ 7.5–7.2 (m, Bzl, Phe ArH), 3.42 (s, NCH_3), 3.22 (s, NCH_3), 2.40 (s, $ArCH_3$), 1.26 (d, Thr CH_3), 0.91 (d, MeVal CH_3), 0.81 (d, MeVal CH_3); FABMS *m/z* (relative intensity) 799.5 (M + 1, 100), 821.4 (M + Na, 10); HRMS calcd for $C_{42}H_{50}N_6O_{10}$ (M + H) 799.3667, found 799.3669.

2,2′-D-Phe$_2$-acetinomycin D (7). A solution of **6** (62 mg, 0.078 mM) in methanol (15 mL) was hydrogenated over 10% PdC (40 mg) at atmospheric pressure for 2 h with stirring. After filtration, the filtrate was added to a solution of 67 mM phosphate buffer (pH 7.1, 20 mL) containing potassium hexacyanoferrate(III) (76.7 mg, 0.23 mM). The mixture was stirred for 10 min at room temperature, and then water (50 mL) was added and the solution was extracted with ethyl acetate (3 × 30 mL). The extracts were washed with water (20 mL) and dried over anhydrous Na_2SO_4. After evaporation of the ethyl acetate, the residue was recrystallized from ethyl acetate to afford 38 mg (72%) of **7** as a red amorphous solid: $[\alpha]^{23}_D$ –277.5° (*c* 0.2, CH_2Cl_2); NMR ($CDCl_3$) δ 8.15 (d, NH), 7.96 (d, NH), 7.87 (d, NH), 7.63 (d, Ar 8-H), 7.35 (d, Ar 7-H), 2.88 (s, NCH_3), 2.89 (s, NCH_3), 2.84 (s, NCH_3), 2.83 (s, NCH_3), 2.53 (s, Ar 6-CH_3), 2.21 (s, Ar 4-CH_3), 1.18 (d, Thr CH_3), 1.15 (d, Thr CH_3), 0.97–0.74 (MeVal CH_3); FABMS *m/z* (relative intensity) 1352 (M + H, 94); HRMS calcd for $C_{70}H_{86}N_{12}O_{16}$ (M + H) 1351.6363, found 1351.6377.

***N*-(Benzyloxycarbonyl)-D-(*O*-methyl)tyrosylprolylsarcosine *tert*-Butyl Ester (8).** A solution of **1** (2.20 g, 5.85 mM) in methanol (30 mL) was hydrogenated over 10% Pd/C (0.56 g) at atmospheric pressure for 2 h with stirring at room temperature. After filtration, the filtrate was evaporated *in vacuo*. To a solution of the residue and *N*-(benzyloxycarbonyl)-D-(*O*-methyl)tyrosine (1.91 g, 5.8 mM) in DCM (20 mL) was added a solution of DCC (1.21 g, 5.85 mM) in DCM (10 mL) at –10 °C. The reaction mixture was stirred for 3 h at –10 °C and then kept overnight in a refrigerator. After removal of DCurea by filtration, the filtrate was evaporated *in vacuo*. The residue was dissolved in ethyl acetate (100 mL), and the solution was washed with 10% citric acid (2 × 30 mL), 1 M $NaHCO_3$ (2 × 30 mL), and water (30 mL) and dried over anhydrous Na_2SO_4. After evaporation of the ethyl acetate *in vacuo*, the residue was purified by the flash column chromatography on silica gel with ethyl acetate–hexane (4:1) to afford 1.79 g (56%) of **8** as a colorless liquid: $[\alpha]^{23}_D$ –55.0° (*c* 1.1, MeOH); NMR ($CDCl_3$) δ 7.33 (s, Bzl ArH), 7.11 (d, Tyr ArH), 6.80 (d, Tyr ArH), 3.77 (s, OCH_3), 3.12 (s, NCH_3), 1.43 (s, OtBu); CIMS in NH_3 *m/z* (relative intensity) 554 (M + H, 45), 571 (M + NH_4, 3); HRMS calcd for $C_{30}H_{39}N_3O_7$ (M + H) 554.2866, found 554.2839.

***N*-(Benzyloxycarbonyl)threonyl-D-(*O*-methyl)tyrosylprolylsarcosine *tert*-Butyl Ester (9).** A solution of **8** (1.79 g, 3.24 mM) in methanol (30 mL) was hydrogenated over 10% Pd/C (0.50 g) at atmospheric pressure for 2 h with stirring. After filtration the filtrate was evaporated *in vacuo*. To a solution of the residue and *N*-(benzyloxycarbonyl)threonine (0.89 g, 3.53 mM) in DCM (20 mL) was added a solution of DCC (0.73 g, 3.53 mM) in DCM (10 mL) at –10 °C. The reaction mixture was stirred for 3 h at –10 °C and then kept overnight in a refrigerator. After removal of DCurea by filtration, the filtrate was evaporated *in vacuo*. The residue was dissolved in ethyl acetate (100 mL), and the solution was washed with 10% citric acid (2 × 30 mL), 1 M $NaHCO_3$ (2 × 30 mL) and water (30 mL) and dried over anhydrous Na_2SO_4. After evaporation of the ethyl acetate *in vacuo*, the residue was purified by flash column chromatography on silica gel with ethyl acetate–methanol (25:1) to afford 1.61 g (72%) of **9** as a colorless solid: $[\alpha]^{23}_D$ –61.1° (*c* 1.0, MeOH); NMR ($CDCl_3$) δ 7.34 (s, Bzl ArH), 7.11 (d, Tyr ArH), 6.79 (d, Tyr ArH), 3.76 (s, OCH_3), 3.08 (s, NCH_3), 1.42 (s, OtBu), 1.14 (d, Thr CH_3); CIMS in NH_3 *m/e* (relative intensity) 655 (M + H, 30), 672 (M + NH_4, 7); HRMS calcd for $C_{34}H_{46}N_4O_9$ (M + H) 655.3343, found 655.3334.

***O*-(*tert*-Butoxycarbonyl)-*N*-methylvalyl-*N*-(benzyloxycarbonyl)threonyl-D-(*O*-methyl)tyrosylprolylsarcosine *tert*-Butyl Ester (10).** To a solution of **9** (1.54 g, 2.35 mM) and *N*-(*tert*-butoxycarbonyl)-*N*-methylvaline (0.76 g, 3.30 mM) in DCM (15 mL) were added DMAP (0.183 g, 1.5 mM) and a solution of DCC (0.83 g, 4 mM) in DCM (20 mL) at 0 °C. The reaction mixture was stirred for 2 h at 0 °C and 14 h at room temperature. After removal of DCurea by filtration, the filtrate was evaporated. The residue was dissolved in ethyl acetate (100 mL), and the solution was washed with 10% citric acid (2 × 30 mL), 1 M $NaHCO_3$ (2 × 30 mL), and water (25 mL) and dried over anhydrous Na_2SO_4. After evaporation of ethyl acetate *in vacuo*, the residue was purified by flash column chromatography on silica gel with ethyl acetate–hexane (5:1) to afford 2.00 g (97%) of **10** as a colorless solid: $[\alpha]^{23}_D$ –67.7° (*c* 1.0, MeOH); NMR ($CDCl_3$) δ 7.34 (s, Bzl ArH), 7.11 (d, Tyr ArH), 6.80 (d, Tyr ArH), 3.76 (s, OCH_3), 3.11 (s, NCH_3), 2.79 (s, NCH_3), 1.48 (s, OtBu), 1.43 (s, OtBu), 1.18 (d, Thr CH_3), 0.93 (d, MeVal CH_3), 0.86 (d, MeVal CH_3); CIMS in NH_3 *m/z* (relative intensity) 868 (M + H, 30), 885 (M + NH_4, 12); HRMS calcd for $C_{45}H_{65}N_5O_{12}$ (M + H) 686.4708, found 868.4733.

***N*-(Benzyloxycarbonyl)threonyl-D-(*O*-methyl)tyrosylprolylsarcosyl-*N*-methylvaline Lactone (11).** A solution of **10** (2.00 g, 2.30 mM) in trifluoroacetic acid (20 mL) was stirred at 0 °C for 4 h. After evaporation of the trifluoroacetic acid *in vacuo*, the residue was dissolved in ethyl acetate (100 mL) then evaporated *in vacuo*. To a solution of the residue in DCM (100 mL) was added triethylamine (0.97 mL, 6.97 mM) at 0 °C, and the mixture was diluted with DCM (1300 mL) then BOP-Cl (1.18 g, 4.62 mM) was added. The reaction mixture was stirred for 5 days at 23 °C. After evaporation of the solvent, the residue was dissolved in ethyl acetate (100 mL) and the solution was washed with 10% citric acid (2 × 25 mL), 1 M $NaHCO_3$ (2 × 25 mL), and water (30 mL). After evaporation of the ethyl acetate, the residue was purified by flash column chromatography on silica gel with ethyl acetate–methanol (20:1) to afford 0.97 g (61%) of **11**, as a colorless solid: $[\alpha]^{23}_D$ –28.4° (*c* 1.0, MeOH); NMR ($CDCl_3$) δ 7.37 (m, Bzl ArH), 7.06 (d, Tyr ArH), 6.78 (d, Tyr ArH), 3.76 (s, OCH_3), 3.42 (s, NCH_3), 3.17 (s, NCH_3), 1.20 (d, Thr CH_3), 0.89 (d, MeVal CH_3), 0.80 (d, MeVal CH_3); CIMS in NH_3 *m/z* (relative intensity) 694 (M + H, 80), 711 (M + NH_4, 2); HRMS calcd for $C_{36}H_{47}N_5O_9$ (M + H) 694.3449, found 694.3429.

(3-(Benzyloxy)-4-methyl-2-nitrobenzoyl)threonyl-D-(*O*-methyl)tyrosylprolylsarcosyl-*N*-methylvaline Lactone (12). A solution of **11** (0.255 g, 0.37 mM) in methanol (15 mL) was hydrogenated over 10% Pd/C (0.15 g) at atmospheric pressure for 2 h with stirring. After filtration the filtrate was evaporated *in vacuo*. To a solution of the residue and 3-(benzyloxy)-4-methyl-2-nitrobenzoic acid (0.116 g, 0.40 mM) in DCM (8 mL) was added a solution of DCC (85 mg, 0.40 mM) in DCM (2 mL) at –10 °C. The reaction mixture was stirred for 3 h at –10 °C and then kept overnight in a refrigerator. After removal of DCurea by filtration, the solution was evaporated *in vacuo*. The residue was dissolved in ethyl acetate (100 mL), and the solution was washed with 10% citric acid (2 × 25 mL), 1 M $NaHCO_3$ (2 × 25 mL), and water (20 mL) and dried over anhydrous Na_2SO_4. After evaporation of the ethyl acetate *in vacuo*, the residue was purified by flash column chromatography on silica gel with ethyl acetate–methanol (10:1) to afford 0.260 g (86%) of **12** as a colorless solid: $[\alpha]^{23}_D$ +4.7° (*c* 1.0, MeOH); NMR ($CDCl_3$) δ 9.72 (d, Thr NH), 7.10 (d, Tyr ArH), 6.80 (d, Tyr ArH), 3.76 (s, OCH_3), 3.42 (s, NCH_3), 3.22 (s, NCH_3), 2.40 (s, Ar CH_3), 1.27 (d, Thr CH_3), 0.91 (d, MeVal CH_3), 0.80 (d, MeVal CH_3); CIMS in NH_3 *m/z* (relative intensity) 829 (M + H, 76), 846 (M + NH_4, 2); HRMS calcd for $C_{43}H_{52}N_6O_{11}$ (M + H) 829.3772, found 829.3789.

2,2′-D-(*O*-Methyl)Tyr$_2$-actinomycin D (13). A solution of **12** (0.100 g, 0.12 mM) in methanol (15 mL) was hydrogenated over 10% Pd/C (40 mg) at atmospheric pressure for 2 h with stirring. After filtration, the filtrate was added to a solution of 67 mM phosphate buffer (pH 7.1, 20 mL) containing potassium hexacyanoferrate(III) (0.118 g, 0.36 mM). The mixture was stirred for 10 min at room temperature, and then water (50 mL) was added and the solution was extracted with ethyl acetate (3 × 30 mL). The extracts were washed with water (20 mL) and dried over anhydrous Na_2SO_4. After evaporation of the ethyl acetate, the residue

was recrystallized from ethyl acetate to afford 50 mg (59%) of **7** as a red amorphous solid: $[\alpha]^{23}_D$ −250.5° (*c* 0.2, MeOH); NMR ($CDCl_3$) δ 8.12 (d, NH), 7.92 (d, NH), 7.65 (d, Ar 8-H), 7.35 (d, Ar 7-H), 7.21 (d, NH), 6.82 (d, NH), 3.80 (s, OCH_3), 2.89 (s, NCH_3), 2.86 (s, NCH_3), 2.85 (s, NCH_3), 2.81 (s, NCH_3), 2.53 (s, Ar-6-CH_3), 2.22 (s, Ar-4-CH_3), 0.73∼0.96 (MeVal CH_3); FABMS *m/z* (relative intensity) 1412 (M + H, 94), 1434 (M + Na, 31); HRMS calcd for $C_{72}H_{90}N_{12}O_{18}$ (M + H) 1411.6574, found 1411.6604.

***N*-(*tert*-Butoxycarbonyl)-D-(*O*-benzyl)tyrosylprolylsarcosine *tert*-Butyl Ester (14).** A solution of **1** (0.77 g, 2.00 mM) in methanol (25 mL) was hydrogenated over 10% Pd/C (300 mg) at atmospheric pressure for 2 h at room temperature. After filtration of the catalyst, the filtrate was evaporated *in vacuo*. To a solution of the residue and *N*-(*tert*-butoxycarbonyl)-D-(*O*-benzyl)tyrosine (0.76 g, 2.0 mM) in DCM (15 mL) was added a solution of DCC (0.43 g, 2.0 mM) in DCM (5 mL) at −10 °C. The reaction mixture was stirred for 3 h at −10 °C and then kept overnight in a refrigerator. After removal of DCurea by filtration, the filtrate was evaporated *in vacuo*. The residue was dissolved in ethyl acetate (85 mL), and the solution was washed with 10% citric acid (2 × 25 mL) 1 M NaHCO3 (2 × 25 mL), and water (25 mL) and dried over anhydrous Na_2SO_4. After evaporation of the ethyl acetate *in vacuo*, the residue was purified by flash column chromatography on silica gel with ethyl acetate–hexane (2:1) to afford 1.03 g (84%) of **14** as a colorless liquid: $[\alpha]^{23}_D$ −59.8° (*c* 1.0, MeOH); NMR ($CDCl_3$) δ 7.38 (m, Bzl ArH), 7.12 (d, Tyr ArH), 6.86 (d, Tyr ArH), 5.04 (s, Bzl CH_2), 3.11 (s, NCH_3), 1.45 (s, OtBu), 1.43 (s, OtBu); FABMS *m/z* (relative intensity) 596 (M + H, 35), 618 (M + Na, 4); HRMS calcd for $C_{33}H_{45}N_3O_7$ (M + H) 596.3336, found 596.3351.

***N*-(Benzyloxycarbonyl)threonyl-D-(*O*-benzyl)tyrosylprolylsarcosine *tert*-Butyl Ester (15).** A solution of **14** (1.00 g, 1.68 mM) in 85% formic acid (40 mL) was stirred at 20 °C for 4 h. After evaporation of the solvent *in vacuo*, the residue was dissolved in 75 mL of ethyl acetate and the solution was washed with 1 M $NaHCO_3$ (2 × 25 mL) and dried over anhydrous Na_2SO_4. After evaporation of the ethyl acetate, to a solution of the residue and *N*-(benzyloxycarbonyl)threonine (0.43 g, 1.7 mM) in DCM (15 mL) was added a solution of DCC (0.35 g, 1.7 mM) in DCM (5 mL) at −10 °C. The reaction mixture was stirred for 3 h at −10 °C and then kept overnight in a refrigerator. After removal of DCurea by filtration, the filtrate was evaporated *in vacuo*. The residue was dissolved in ethyl acetate (80 mL), and the solution was washed with 10% citric acid (2 × 25 mL), 1 M $NaHCO_3$ (2 × 25 mL), and water (25 mL) and dried over anhydrous Na_2SO_4. After evaporation of of the ethyl acetate, 0.81 g (66%) of **15** was afforded as a colorless solid: $[\alpha]^{23}_D$ −58.5° (*c* 1.0, MeOH); NMR ($CDCl_3$) δ 7.37 (m, Bzl ArH), 7.11 (d, Tyr ArH), 6.67 (d, Tyr ArH), 5.13 (s, Bzl CH_2), 5.03 (s, Bzl CH_2), 3.09 (s, NCH_3), 1.43 (s, OtBu), 1.15 (d, Thr CH_3); FABMS *m/z* (relative intensity) 731 (M + H, 40), 753 (M + Na, 12); HRMS calcd for $C_{40}H_{50}N_4O_9$ (M + H) 731.3656, found 731.3670.

***O*-(*tert*-Butoxycarbonyl)-*N*-methylvalyl-*N*-(benzyloxycarbonyl)threonyl-D-(*O*-benzyl)tyrosylprolylsarcosine *tert*-Butyl Ester (16).** To a solution of **15** (0.77 g, 1.05 mM) and *N*-(*tert*-butoxycarbonyl)-*N*-methylvaline (0.35 g, 1.51 mM) in DCM (10 mL) were added DMAP (90 mg, 0.74 mM) and a solution of DCC (0.41 g, 2.0 mM) in DCM (5 mL) at 0 °C. The reaction mixture was stirred for 2 h at 0 °C and then 14 h at room temperature. After removal of DCurea by filtration, the filtrate was evaporated. The residue was purified by flash column chromatography on silica gel with ethyl acetate–hexane (4:1) to afford 0.91 g (91%) of **16** as a colorless solid: $[\alpha]^{23}_D$ −62.1° (*c* 0.9, MeOH); NMR ($CDCl_3$) δ 7.36 (m, Bzl ArH), 7.12 (d, Tyr ArH), 6.86 (d, Tyr ArH), 5.11 (s, Bzl CH_2), 5.04 (s, Bzl CH_2), 3.11 (s, NCH_3), 2.79 (s, NCH_3), 1.45 (s, OtBu), 1.43 (s, OtBu), 1.20 (d, Thr CH_3), 0.93 (d, MeVal CH_3), 0.86 (d, MeVal CH_3); FABMS *m/z* (relative intensity) 944 (M + H, 14), 966 (M + Na, 15); HRMS calcd for $C_{51}H_{69}N_5O_{12}$ (M + H) 944.5021, found 944.5008.

***N*-(Benzyloxycarbonyl)threonyl-D-(*O*-benzyl)tyrosylprolylsarcosyl-*N*-methylvaline Lactone (17).** A solution of **16** (0.90 g, 0.95 mM) in trifluoroacetic acid (10 mL) was stirred at 0 °C for 4 h. After evaporation of the trifluoroacetic acid *in vacuo*, the residue was dissolved in ethyl acetate (70 mL) and the fluid was evaporated *in vacuo*. To a solution of the residue in DCM (100 mL) was added triethylamine (0.40 mL, 2.9 mM) at 0 °C, the mixture was diluted with DCM (650 mL), then BOP-Cl (607 mg, 2.4 mM) was added. The reaction mixture was stirred for 5 days at room temperature. After evaporation of the solvent, the residue was dissolved in ethyl acetate (80 mL) and the solution was washed with 10% citric acid (2 × 20 mL), 1 M $NaHCO_3$ (2 × 20 mL), and water (25 mL) and dried over anhydrous Na_2SO_4. After evaporation of the ethyl acetate, the residue was purified by flash column chromatography on silica gel with ethyl acetate–methanol (20:1) to afford 405 mg (55%) of **17** as a colorless solid: $[\alpha]^{23}_D$ −26.2 (*c* 1.0, MeOH); NMR ($CDCl_3$) δ 7.37 (m, Bzl ArH), 7.03 (d, Tyr ArH), 6.85 (d, Tyr ArH), 5.20 (d, Bzl CH_2), 5.03 (s, Bzl CH_2), 3.42 (s, NCH_3), 3.17 (s, NCH_3), 1.21 (d, Thr CH_3), 0.89 (d, MeVal CH_3), 0.79 (d, MeVal CH_3); FABMS *m/z* (relative intensity) 770 (M + H, 100), 792 (M + Na, 30); HRMS calcd for $C_{42}H_{51}N_5O_9$ (M + H) 770.3765, found 770.3780.

(3-(Benzyloxy)-4-methyl-2-nitrobenzyl)threonyl-D-tyrosylprolylsarcosyl-*N*-methylvaline Lactone (18). A solution of **17** (250 mg, 0.32 mM) in methanol (20 mL) was hydrogenated over 10% Pd/C (250 mg) at atmospheric pressure for 5 h with stirring. After filtration the filtrate was evaporated *in vacuo*. To a solution of the residue and 3-(benzyloxy)-4-methyl-2-nitrobenzoic acid (98 mg, 0.34 mM) in DCM (10 mL) was added a solution of DCC (70 mg, 0.34 mM) in DCM (2 mL) at −10 °C. The reaction mixture was stirred for 3 h at −10 °C and then kept overnight in a refrigerator. After removal of DCurea by filtration, the solution was evaporated *in vacuo*. The residue was purified by flash column chromatography on silica gel with ethyl acetate–methanol (20:1) to afford 182 mg (69%) of **18** as a colorless solid: $[\alpha]^{23}_D$ −2.4° (*c* 0.5, MeOH); NMR ($CDCl_3$) δ 9.69 (d, Thr NH), 7.40 (m, Bzl ArH), 6.98 (d, Tyr ArH), 6.72 (d, Tyr ArH), 5.00 (d, Bzl CH_2), 3.38 (s, NCH_3), 2.38 (s, $ArCH_3$), 1.26 (d, Thr CH_3), 0.90 (d, MeVal CH_3), 0.79 (d, meVal CH_3); FABMS *m/z* (relative intensity) 815 (M + H, 100), 837 (M + Na, 38); HRMS calcd for $C_{42}H_{50}N_6O_{11}$ (M + H) 815.3616, found 815.3611.

2,2′-D-Tyr$_2$-actinomycin D (19). A solution of **18** (58 mg, 0.07 mM) in methanol (15 mL) was hydrogenated over 10% Pd/C (50 mg) at atmospheric pressure for 2 h with stirring. After filtration the filtrate was added to a solution of 67 mM phosphate buffer (pH 7.1, 15 mL) containing $K_3Fe(CN)_6$ (68 mg, 0.21 mM). The mixture was stirred for 20 min at room temperature, and then water (30 mL) was added and extracted with ethyl acetate (3 × 25 mL). The ethyl acetate layer was washed with water (15 mL) and dried over anhydrous Na_2SO_4. After evaporation of the ethyl acetate, the residue was recrystallized from ethyl acetate to afford 28 mg (57%) of **19** as a red amorphous solid: $[\alpha]^{23}_D$ −261.4° (*c* 0.22, MeOH); NMR ($CDCl_3$) δ 8.31 (d, NH), 7.90 (d, NH), 7.78 (d, NH), 7.61 (d, NH), 7.57 (d, Ar 8-H), 7.37 (Ar 7-H), 7.14 (d, Tyr ArH), 7.06 (d, Tyr ArH), 6.77 (d, Tyr ArH), 6.69 (d, Tyr ArH), 2.91 (s, NCH_3), 2.89 (s, NCH_3), 2.87 (s, NCH_3), 2.82 (s, NCH_3), 2.51 (s, Ar 6-CH_3), 2.22 (s, Ar 4-CH_3), 1.25 (d, Thr CH_3), 0.78–1.00 (MeVal CH_3); FABMS *m/z* (relative intensity) 1384 (M + H, 90), 1406 (M + Na, 50); HRMS calcd for $C_{70}H_{87}N_{12}O_{18}$ (M + H) 1383.6261, found 1383.6288.

X-ray Crystallography. Compound **13** was recrystallized from ethyl acetate solution in a refrigerator. Since the crystals diffracted very weakly and decayed relatively quickly under X-ray exposure at room temperature, the X-ray diffraction experiment was carried out at low temperature (113 K). Approximately 200 μL of Paraton N oil was dropped on the orange-red prism crystals of **13**. A crystal having approximate dimensions of 0.40 × 0.40 × 0.60 mm was scopped with a glass fiber under a microscope and was immediately frozen on an X-ray diffractometer under a cold nitrogen stream (at 113 K). All measurements were on a Rigaku AFC5R diffractometer with graphite-monochromated Cu Kα radiation (λ = 1.5418 Å) at 113 ± 2 K and a 12 kW rotating anode generator. Cell constants and orientation matrices for data collection were obtained from a least-squares refinement using the setting angles of 25 carefully centered reflections in the range $14° < 2\theta < 21°$. The crystal belongs to a tetragonal system of $a = b = 21.352(6)$ and $c = 44.525(9)$ Å. On the basis of systematic absences of $h00$, $h \neq 2n$, and $00l$, $l \neq 4n$, the space group is $P4_12_12$ or its enantiomorph ($P4_32_12$). From the successful solution and refinement of the structure, the space group was determined to be $P4_12_12$ (No. 92) and $Z = 8$. The data were collected using the ω scan technique to a maximum 2θ value of 51° (1.8-Å resolution). ω scans of several intense reflections, made prior to data collection, had an average width at half-height of 0.45∼0.55° with a take off angle of 6.0°. Scans of (1.26 + 0.30 tan θ)° were made at a speed of 1.0 deg/min (in ω). Stationary background counts were recorded on each side of the reflection. The ratio of peak counting time to background counting time was 2:1. The diameter of the incident beam collimator was 0.5 mm, and the crystal to detector distance was 285.0 mm. The intensities of three representative reflections that were measured after every 150 reflections remained constant throughout data collection, indicating crystal and electronic stability (no decay correction was applied). Empirical absorption corrections, based on azimuthal scans of several reflections, were applied on all data. The data were corrected for Lorentz and polarization effects. Of the 1165 reflections that were collected, 1114 were unique.

The molecular replacement method was applied to solve the structure, using 431 reflection data in the resolution range 25–2.0 Å ($F_o > 10\sigma(F_o)$)

by using the X-PLOR.[39] An initial attempt using a classic cross-rotation function with the crystal structure of AMD itself as a search model was not successful. The direct rotation function followed by the Patterson correlation refinement as proposed by Brünger[40] was applied. This method gave 23 distinguishable molecular orientations. All orientations were tested by the R-factor search procedure in both space groups ($P4_12_12$ and $P4_32_12$). The lowest R-factor of 0.47 was found with the 20th orientation of the space group $P4_12_12$. The orientation and translation parameters of the model were further tuned by varying the small step sizes of parameters around this orientation and position. The model was then refined by the rigid-body least-squares procedure, treating each of a phenoxazone ring and two depsipeptide rings as rigid groups to give an R-factor of 0.40. Positional refinement of each atom reduced the R-factor to 0.34. At this stage, two methoxyphenyl groups were clearly located in a $2F_o - F_c$ map. The individual non-hydrogen atoms were restrained to have idealized bond distances and angles and refined by the full-matrix least-squares method, minimizing $[\sum w_f(|F_o| - |F_c|)^2 + \sum w_d(|D_o| - |D_c|)^2]$.[41] Solvent atoms, mainly water and disordered ethyl acetate molecules, were located in difference maps and were introduced into refinement. Since most solvent atoms were heavily disordered, the occupancy factors were only varied and positional and thermal parameters were fixed on the positions found in the difference maps and 30.0 Å,^{2} respectively. Neutral-atom scattering factors were taken from the *International Tables of X-ray Crystallography* (1974).[42] The final cycle of full-matrix least-squares refinement was based on 803 observed reflections ($I > 1.00\sigma(I)$) for 150 non-hydrogen atoms (102 atoms of compound **13** and 48 disordered waters) and converged with $R = \sum||F_o| - |F_c||/\sum|F_o| = 0.19$ and $R_w = [\sum w(|F_o| - |F_c|)^2/\sum wF_o^2]^{1/2} = 0.15$.

UV/Vis Spectrum Measurements. UV/vis absorption spectra were measured on a JASCO V-560 double beam spectrometer. Samples of oligonucleotides (15 μM) d(GAAGCTTC)$_2$ and d(GTTGCAAC)$_2$ were synthesized by a Cruachem PS250 DNA/RNA synthesizer using the protocol provided from the company. After the deprotection procedure, the crude oligonucleotides were purified by a reverse-phase HPLC using C_{18} columns. Stock solutions of these oligomers (400 μM) were prepared in a binding buffer (45 mM Tris-HCl (pH 8.0), 1.25 mM $MgCl_2$, 2.5 mM NaF, and 6.0 mM KCl). All binding experiments were carried out in this buffer. Concentrations of these oligomers (single strand) were determined from their absorbances at 260 nm after melting using the following extinction coefficients, ϵ_{260}, of oligonucleotides: 72.5×10^3 M^{-1} cm^{-1} for d(GAAGCTTC) and 76.1×10^3 M^{-1} cm^{-1} for d(GTTGCAAC).[43] Calf thymus DNA (Sigma) was sonicated and purified to eliminate residual protein by repeated phenol extraction and then ethanol precipitation. Poly(dA-dT) and poly(dG-dC) were purchased from Boehringer Mannheim GmbH and Sigma, respectively, and were not further purified. Stock solutions of these DNA's (1 mM in bp) were prepared in the binding buffer on the basis of ϵ_{260}(calf thymus)[22,44] = 1.25×10^4 M^{-1} cm^{-1}, ϵ_{254}(poly(dG-dC)) = 1.68×10^4 M^{-1} cm^{-1}, and ϵ_{260}(poly(dA-dT)) = 1.30×10^4 M^{-1} cm^{-1}. The concentrations of AMD and AMD analogue solutions were determined using an extinction coefficient of 2.45×10^4 M^{-1} cm^{-1} at 440 nm.[28]

Difference spectra of drugs with oligonucleotides were obtained by the following procedure. After measurement of the visible spectrum of a drug solution (<4.3 μM) in binding buffer (pH 8.0), the drug solution was placed into a reference cuvette and the base line of the double beam spectrometer was determined with two cuvettes. A small aliquot of a known concentration of stock oligonucleotide solution was added to a sample cuvette, while the same amount of buffer was added to the reference cuvette. After a 10–15-min wait, difference spectra were measured. This procedure was repeated four times so that four difference spectra were measured at four different DNA concentrations. All experiments were carried out at 10 °C. The absorbances of visible spectra and difference spectra were taken at 2-nm intervals for use of the binding constant calculation.

The absorption spectra of the drug during titration with poly-DNA were obtained in order to find out the binding character of drug to poly-DNA. After the absorbance of 1.0 mL of the drug solution (1 μM) in the binding buffer was measured from 600 to 350 nm at room temperature, 5 μL of poly-DNA stock solution was added into the sample cuvette and spectra were measured after 15 min or more. This procedure was repeated six times so that six spectra were measured at six different DNA concentrations (5, 10, 15, 20, 25, and 30 μM bp). The absorbances of visible spectra were output at every 2-nm interval. Dilution factors were applied to all spectra.

DNA Melting Profile Measurements. A JASCO HMC-358 constant-temperature cell hold connected with a NESLAB RTE-111 bath circulator was used to obtain the melting profiles of DNA. A 10-μL portion of calf thymus DNA or poly-DNA solution (1.0 mM bp) was added into the sample cuvette containing 990 μL of 0.25 mM phosphate buffer (pH 7.0, 0.5 mM NaCl) in the presence or absence of the drug, and the absorption at 260 nm was measured from 40 to 85 °C. The cuvette temperature was monitored by putting a thermocouple directly in the cuvette and increased approximately 0.5 deg/min.

Water Solubility Measurements. AMD and AMD analogues were dissolved in binding buffer (pH 8.0) until the compounds were saturated. After centrifugation, the concentrations of drugs were determined spectrophotometrically.

RNA Synthesis Inhibition Assay. The inhibitory activities of AMD and AMD analogues on RNA synthesis *in vitro* were examined using calf thymus DNA and *E. coli* RNA polymerases. The RNA polymerase assay was carried out by a modification of the method of Grula and Weaver[45] as follows:

(1) Prepare the RNA polymerase assay mix which contains 6.0 mM $MnCl_2$, 12 mM NaF, 28.7 mM KCl, 1.44 mg/mL GTP, 1.68 mg/mL ATP, 1.44 mg/mL CTP, 0.06 mg/mL UTP, 1.2 mg/mL bovine serum albumin, 216 mM tris-HCl (pH 8.0), 0.48 mM spermine, 2.8 mM DTT, and 60 μCi/mL ^{3}H-UTP.

(2) Place 10- × 75-mm glass test tubes in ice and add 10 μL of 1.0 mg/mL calf thymus DNA and 75 μL of water.

(3) Add 5 μL of AMD or AMD analogue stock solutions (3, 6, 9, 18, and 36 μg/mL in MeOH). The final drug concentrations are 0.125, 0.25, 0.5, 1.0, and 2.0 μg/mL.

(4) Add 5 μL of 16 μg/mL RNA polymerase (*E. coli*, from Sigma). This gives 2000–3000 cpm/reaction.

(5) Add 25 μL of RNA polymerase assay mix.

(6) Incubate the reactions at 37 °C for 30 min.

(7) Spot 100 μL of each reaction on a DE81 filter (DEAE-cellulose ion exchanger from Whatman) and dry for 15 min.

(8) Wash four times for 10 min in 5% Na_2HPO_4.

(9) Rinse two times with water.

(10) Rinse with 95% ethanol and dry in an oven.

(11) Count ^{3}H-UTP incorporation with a liquid scintillation counter (Beckman LS 1800).

All measurements were carried out in duplicate.

Acknowledgment. The authors express their thanks to Dr. Rui Wang for his contribution to the synthesis of Phe-AMD and to Mrs. Li Wen for DNA synthesis and purification. This work has been supported by grants from the National Institutes of Health, the Kansas Health Foundation, and the Marian Merrell Dow Foundation.

Supplementary Material Available: Tables of positional and thermal parameters of compound **13** (7 pages); tables of observed and calculated structure factors (8 pages). This material is contained in many libraries on microfiche, immediately follows this article in the mcirofilm version of the journal, and can be ordered from the ACS; see any current masthead page for ordering information.

(39) Brünger, A. T. *X-PLOR 3.1. A System for X-ray Crystallography and NMR*; Yale University Press: New Heaven, London, 1993.
(40) Brünger, A. T. *Acta Crystallogr.* **1990**, *A46*, 46–57.
(41) Takusagawa, F. CRLS: Constrained-Restrained Least-Squares. Technical Report ICR-1982-0001-0002-0001; The Institute for Cancer Research: Philadelphia, PA, 1982.
(42) Cromer, D. T.; Waber, J. T. *International Tables for X-ray Crystallography*: Ibers, J. A., Hamilton, W. C., Eds.; The Kynoch Press: Birmingham, England, 1974; Vol. IV, pp 99–101.
(43) Cantor, C. R.; Warshaw, M. M. *Biopolymer* **1970**, *9*, 1059–1077.
(44) Winkle, S. A.; Krugh, T. R. *Nucleic Acids Res.* **1981**, *9*, 3175–3186.
(45) Grula, M. A.; Weaver, R. F. *Insect Biochem.* **1981**, *11*, 149–154.
(46) Dickerson, R. E.; Kopka, M. L.; Pjura, P. *Chem. Scr.* **1986**, *26B*, 139–145.
(47) Angerman, N. S.; Victor, T. A.; Bell, C. L.; Danyluk, S. S. *Biochemistry* **1972**, *11*, 2402–2411.